University of Cincinnati

Date: 5/17/2012

I, Rutvij Kotecha , hereby submit this original work as part of the requirements for the degree of Master of Science in Materials Science.

It is entitled:

Atmospheric Pressure Microwave Plasma for Materials Processing and Environmental Applications

Student's name: **Rutvij Kotecha**

This work and its defense approved by:

Committee chair: Vesselin Shanov, PhD

Committee member: Dale Schaefer, PhD

Committee member: Mark Schulz, PhD

2763

UNIVERSITY OF Cincinnati

Atmospheric Pressure Microwave Plasma for Materials Processing and Environmental Applications

A thesis submitted to the Graduate School

of the University of Cincinnati

in partial fulfillment of the requirements for the degree of

MASTER OF SCIENCE

in Materials Science & Engineering

in the School of Energy, Environment, Biological & Medical Engineering

(SEEBME)

by

Rutvij Kotecha

Bachelor of Technology – Motilal Nehru National Institute of Technology, India

2008

Committee Chair: Professor. Vesselin Shanov

Thesis Abstract

This thesis summarizes the research on two novel applications of Atmospheric Pressure Microwave Plasma (APMP) system, i.e. – (i) functionalization of carbon nanotube (CNT) materials, and (ii) disinfection of water contaminated by *Bacillus globigii* spores.

During the first phase of the research, the APMP system was reengineered for functionalization of CNT ribbons – a unique nanomaterial synthesized at Nanoworld Labs at UC. The ribbon bridges the dimensional and property gap between carbon nanotubes and their macro scale applications, such as light weight composites, biomedical, electronic devices, etc. However in order to improve the performance of CNT ribbons, they have been functionalized with fluorocarbon films using APMP system.

Time-of-flight secondary ion mass spectrometry (TOF-SIMS) characterizations have indicated the presence of CF_2 as a repeating unit in the film. Further, atomic concentration of C, F and O and the type of bonding in film were studied through X-ray Photoelectron Spectroscopy (XPS).

The functionalization on the ribbons may improve its performance in light weight composites and other macro-scale applications.

During the second phase of the research, applicability of APMP system for decontamination of water containing *Bacillus globigii* spores was explored. Water

samples were treated by various plasma gas (He + 1% H_2, He, O_2 and N_2) effluents. The magnetron power level was varied between 250 W to 400 W. The results obtained indicate that He + 1% H_2 and O_2 as plasma gases were more effective than He or N_2. Best disinfection results with APMP were obtained when the incident microwave power level was 325 W.

Based on literature review and experimental observations, it is has been concluded that UV and reactive oxygen species are the most important contributing factors for elimination of *B. globigii* spores.

These experiments indicate that APMP system can be successfully employed a variety of problems in materials processing and environmental engineering.

This page has been left blank intentionally.

Dedicated to my mentors – My parents, Prof. Ajay Patwardhan, Prof. Manoj Gupta, Prof. Charles Matthews and Mr. Tom Kruer.

Acknowledgements

As I approach the flag end of my MS degree, I realize that my success as a graduate student has been due to the support endowed to me by my advisor, family, friends, departmental staff, grant administrators and the Almighty. Thank you very much for partaking in my mission!

My journey as a graduate student became fulfilling due to my advisor Prof. Vesselin Shanov's constant guidance and encouragement. I am highly obliged to him for helping me remain financially self-reliant through a Graduate Research Assistantship. I would not have been selected for the prestigious internship with Ohio Board of Regents without his recommendation. I shall always cherish the liberty that he granted me in engineering the plasma system, vacuum chamber and many other experimental facilities.

I was able to implement most of my engineering ideas due to the support and keen insight of Mr. Doug Hurd, Chief Machinist at University of Cincinnati. I have great respect for his profound engineering skills, and ability to understand the mechanism of devices and to take concepts from ideation stage to product. I am also very thankful to Mr. Terry Craycraft for being available to repair the plasma system at crucial times.

I am grateful to Drs. Peter Kosel, George Sorial, Dion Dionysiou, David Wendell, William Vanooij, Dale Schaefer, Mike Sitko and Jeff Szabo for their valuable time and input. Their guidance helped me look at my research problem from a different angle.

I am indebted to Dr. Govindaraju Nirmal for helping me understand the concepts of plasma and materials engineering. Our discussions have welded my bond with him as a friend, mentor and teacher. His guidance was indispensable in shaping my resume, cover letter, statement of purpose (SOP) and research presentations.

I shall always remember my research lab mates for being so cooperative and supportive at all times. Their presence made working in the lab very cheerful and enjoyable.

I am fortunate to have Bineyam Mezgebe and A. Davison Gilpin as my friends, for their help was vital in carrying out some of the key experiments.

During the few years that I have spent as a student at the University of Cincinnati, I had the opportunity to interact with thousands of students from all across the globe. Some of them have left a footprint in my heart that I shall always cherish them. The fond memories that I have shared with Bala Padmini Lingaraju, Vibhor Chaswal, Siddharth Pradhan (soon to be a renowned Dr. and professor), Shaleen Bhatia, Andrea Young Lee, Durgesh Rai, Aniruddha and Shruti Deshpande, Jaspreet Singh, Nimita Dave, Pravahan and Mithilesh Salunke, Jimmy Longun, A. Davison Gilpin, Bing Han, Sandeep Singh, Hardik Mehta and many others, are hard to forget.

When I take the walk to receive my degree, I shall remember that the milestones that I have accomplished wouldn’t have been possible without the gracious support of so

many kind hearted individuals. Thank you everyone for helping me achieve my goal! I hope you give me a chance in the future to return the favor.

TABLE OF CONTENTS

List of Figures

List of Tables

Glossary

APMP	Atmospheric Pressure Microwave Plasma
B. globigii	*Bacillus globigii*
BWA	Biological Warfare Agents
CNT	Carbon Nanotube
CVD	Chemical Vapor Deposition
DI	Deionized water
DWNT	Double walled carbon nanotube
ICP-OES	Inductively coupled plasma - optical emission epectrometer
ITO	Indium tin oxide (coated glass)
Lpm	Liters per minute
MFC	Mass flow controllers
MUV	Middle UV (300 – 200 nm)
MWNT	Multi walled carbon nanotube
OES	Optical emission spectrometer
PDA	1H,1H,2H,2H-Perfluorodecyl acrylate
PFH	Perfluoroheptane
PFMCH	Perfluoro(methylcyclohexane)
RGA-QMS	Residual gas analyzer – quadrupole mass spectrometer
RNS	Reactive nitrogen species
ROS	Reactive oxygen species
sccm	Standard cubic centimeter
SEM	Scanning electron microscope
SWNT	Single walled nanotube
TSA	Trytic (Trypticase) Soy Agar
UHP	Ultra high purity
UVB	Ultraviolet B (315 – 280 nm)
UVC	Ultraviolet C (280 – 100 nm)

Section 1: Introduction to Plasma and Plasma Systems

Plasma is a mixture of neutral gas atoms/molecules, ions of plasma gas atoms/molecules and electrons. It has also been defined as: "A *quasi-neutral* gas of charged and neutral particles characterized by a collective behavior."[1] It has gained significant importance in the last few years due to its versatility in materials synthesis, materials processing and application in biomedical industry.

1. Application of plasma systems

Some of the key applications of plasma system are as follows:

- Material synthesis
    - *Carbon Nanotubes*

Plasma enhanced Chemical Vapor Deposition (PE-CVD) of carbon nanotubes results in vertically aligned carbon nanotubes.[2, 3] Additionally, CNT can be grown perpendicular to the substrate, irrespective of the orientation or geometry of the substrate.[4] PE-CVD enables synthesis of CNT at a lower temperature as compared to CVD technique.[3, 5]

- *Diamond thin films*

Due to the unique properties of diamond (eg – mechanical hardness of 90 GPa, electrical resistivity[6] : 10^{13} Ω-cm etc), it has gained significant industrial importance. However, in order to synthesize diamond synthetically, very high pressure[1] (several hundred thousand bars) and temperature[1, 6] (2000 K – 3773 K) - have to be applied. By using PE-CVD, diamond can be synthesized at 0.013 – 0.26 bar and 850 – 950°C [1].

- Functionalization of materials
    - Etching

      In VLSI processing, it is crucial to etch the substrate anisotropically. As compared to chemical etching, plasma offers benefits in anisotropic etching of surfaces in terms of geometry and dimension of the features.[1] In addition, plasma processing does not require any special chemical waste disposal.

- Environmental application
    - *Disinfection of air, water and pollutants*

Due to the development of atmospheric pressure plasma system, there is a reduced reliance on vacuum chambers.[7, 8] As a result, plasma system is being explored as a tool for disinfecting chemical and biological warfare agents in air, water or solid surface.[9] In addition, plasmas are commonly used for sterilizing medical equipments.[10]

2. Plasma generation

Plasma can be generated at in a chamber at low pressure or without a chamber at atmospheric conditions. Atmospheric pressure plasma systems are of particular interest because they are economical as compared to vacuum plasma systems and they do not require complex chambers.[11, 12] Following are some of the popular techniques for generating plasma.

- *DC Glow Discharge*

In a glow discharge plasma, DC voltage is applied to the electrode which are enclosed in an tube at low pressure. Figure 1 displays a schematic of DC glow discharge plasma systems.

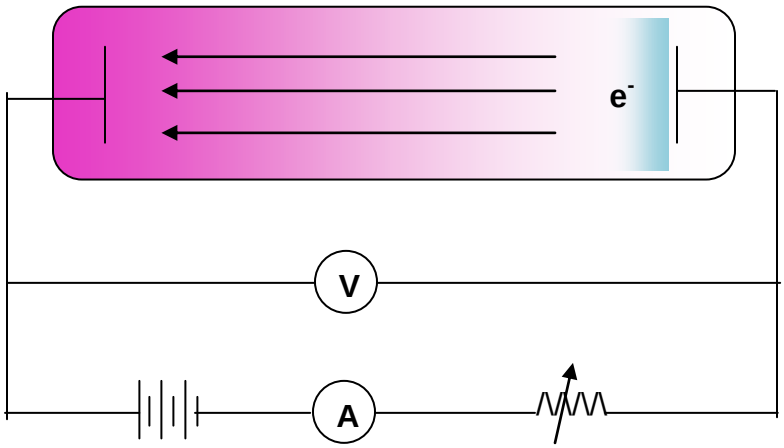

Figure 1 Schematic of DC glow discharge tube.

- *Microwave plasma*

  - In an atmospheric pressure microwave plasma system, microwaves (frequency: 2.45GHz) are generated by the magnetron, which propagate through a waveguide to the quartz torch (also known as the plasma torch).[13] The waveguides are rectangular tubes and have high conductivity. Plasma is sustained by coupling microwave energy to the plasma gas through an applicator.[1]

3. Working of ASTEX plasma system

The research described in this thesis has been performed by using an atmospheric pressure microwave plasma system from ASTEX (subsidiary of MKS Instruments, Inc.,

model number: AX2115). Figure 2 is an image of APMP system used for this research. Figure 3 shows a general schematic of the plasma system used for experiments. The plasma system has a non-porous alumina rod (refer to Figure 3) of 1/4" diameter (from McMaster Carr, product number: 87065K46) has been used.

The SmartMatch^{TM} is a device mounted on the waveguide to maximize the microwaves incident on the quartz torch by adjusting three metallic stubs to minimize the reflected microwaves from the surfaces. The microprocessor (in SmartMatch^{TM}) decides the position of the stubs based on the input from detector module and an algorithm.[14] The microwaves interact with the gas (He + 1% H_2, He, N_2 or O_2) to produce plasma.

Safety considerations

a) After making modifications or repairs in the plasma system, suspicious regions such as flanges, openings etc were inspected for microwave leaks using a leak detector from Holaday Industries, Inc. (model no: 1501). As per the guidelines, the microwave plasma system was not operated if the intensity of microwave leak was greater than 2 mW/cm^2.
b) It was ensured that there was no H_2 leak between the cylinder and plasma torch.
c) Protective glasses are worn at all times to protect the eyes from UV radiation.

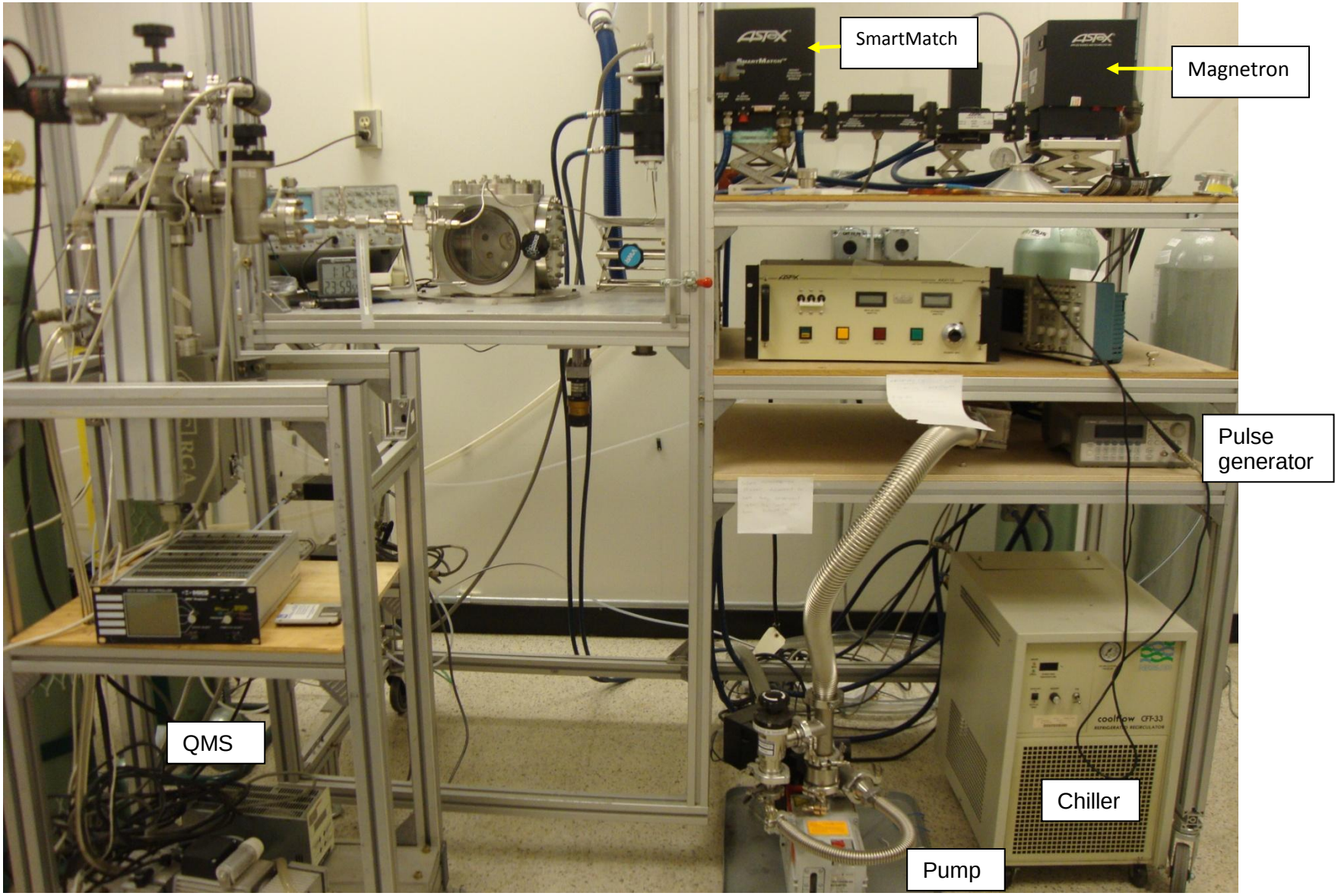

Figure 2 APMP system used for functionalization of materials processing and environmental application.

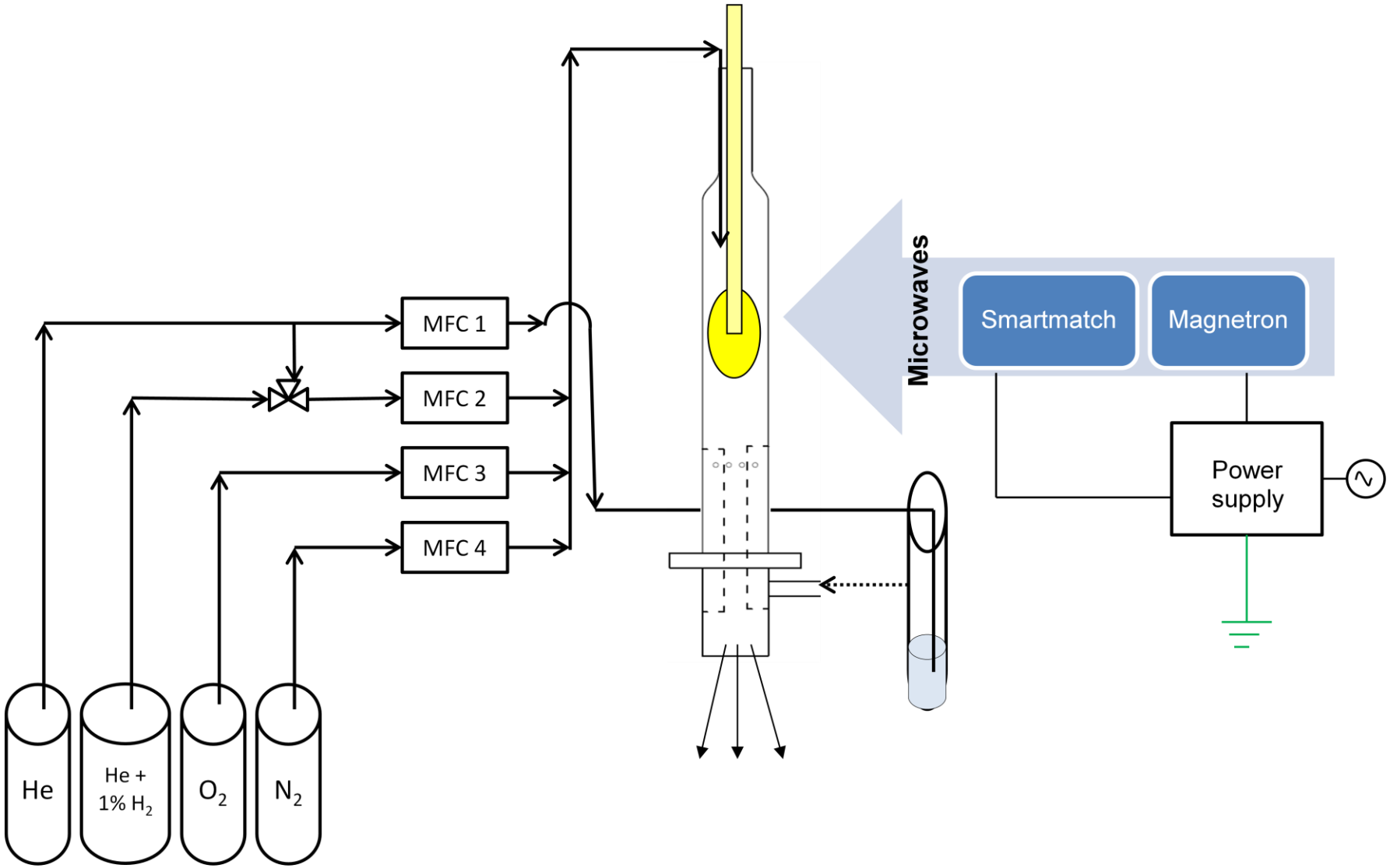

Figure 3 Schematic of Atmospheric Pressure Microwave Plasma system.

Section 2: Application of Atmospheric Pressure Microwave Plasma for Functionalization of Carbon Nanotube Materials

Abstract

This section of the thesis deals with application atmospheric pressure plasma system (described in Section 1) for functionalizing carbon nanotube ribbons. CNT arrays were synthesized by Chemical Vapor Deposition (CVD) and spun into ribbons, which were coated using atmospheric pressure microwave plasma system. Time-of-flight secondary ion mass spectrometry (TOF-SIMS) characterization of CNT ribbons indicated the presence of polymer films with CF_2 as a repeat unit. Atomic concentration of C, F and O in the coated films was estimated from X-ray photoelectron spectroscopy (XPS) data. Type of bonding between the elements in the coated films was studied by curve fitting of C 1s XPS spectra.

Results of the experiments mentioned in this section have been published in: Materials Research Society 2011 Symposium Proceedings Vol. 1 (DOI: 10.1557/opl.2011.1128).

1. Introduction

1.1. Carbon Nanotubes

Carbon nanotubes (CNT) are "seamless cylindrical shells of graphitic sheets".[15] CNTs were first discovered by Sumio Iijima in 1991.[16] In CNT carbon atoms have sp^2 hybridization.[15]

CNT can be singlewalled (SWNT) or multiwalled (MWNT).[17] Double walled CNT, which are a special case of MWNT, are known for their chemical stability and under inert environment they can withstand temperatures up to 2000 °C.[18] Generally the spacing between the consecutive walls of nanotubes is in the order of 0.34 nm.[18] Figure 4 represents the various chiral structures possible for SWNT.

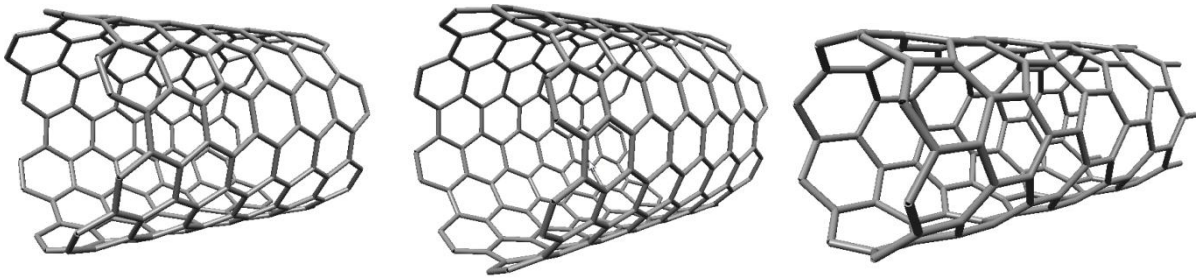

(a) (b) (c)

Figure 4 Configuration of SWNT. (a) Chiral: (8,6), (b) Arm-chair (8, 8), and (c) Zig-zag (8, 0). Numbers in the bracket represent (n, m) value of the vector. Modeling done using Nanotube Modeler Version 1.7.3.

Chiral vector is represented by: $C_h = n^*\widehat{\mathbf{a1}} + m^*\widehat{\mathbf{a2}}$ and is graphically represented in Figure 5, where $0 \leq |m| \leq n$. The angle $\theta = \tan^{-1}(n\sqrt{3}/(2m+n))$, where $0 \leq \theta \leq 30°$.

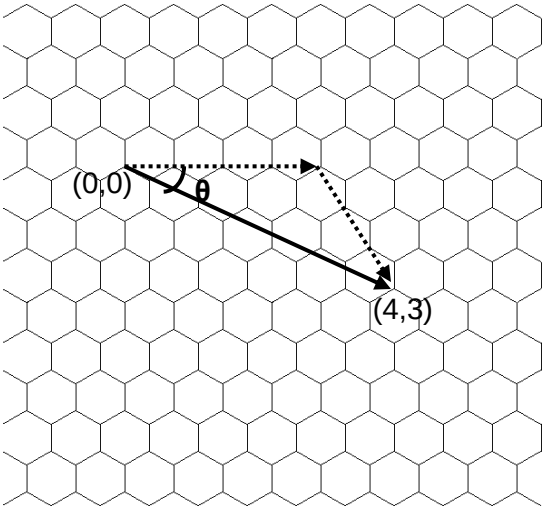

Figure 5 Representation of chiral vector.

Single-walled CNT have Young's modulus of approximately 1.8 TPa.[19] Due to high Young's modulus and low density of 1.4 g/cm^3,[20] CNT are ideal for light weight composite applications.[19, 21] CNT have also been regarded as a potential candidate for various applications such as: hydrogen storage, ballistic protection shields, EMI shielding, nanoelectromechanical systems (NEMS), etc.[16, 22, 23]

1.2. Translating properties of CNT from nano to macro scale

However, there is a major limitation in translating their properties from nano to macro scale applications.[24] In order to overcome these limitations, research has been performed to synthesize nanotube materials by wet spinning, spinning from furnace, spinning from deposited CNT forest and buckypaper.[20] The strength of the yarn obtained by wet spinning of single-walled nanotubes is approximately one-tenth the order strength of single-walled nanotube.[25]

Of late, CNT ribbons have been synthesized directly from CNT arrays by pulling one end of the CNT array to form a continuous ribbon. A thread is obtained by twisting the ribbon while it is being pulled from the array. In CNT ribbons, CNT are parallelly aligned to one another and held together by Vander Waals force. Therefore CNT ribbons have been preferred for this research over CNT powdered form.

1.3. Rationale behind functionalization of CNT ribbons

Nanotube threads and ribbons are of particular interest due to their potential application in in-vivo and in-vitro biomedical applications, supercapacitors and light weight composite materials. However the surface properties of CNT material are not suitable for directly using them for various applications.[26] Therefore, these materials have to be functionalized before they can be used. Keeping in mind the application of functionalized CNT ribbons in composites and biomedical applications, fluorine is the desired element for functionalization on the ribbons.

1.4. Characteristics of fluorocarbon films and their key applications

Fluorocarbon coatings (and Teflon particularly) are of interest due to their chemical inertness, mechanical and thermal stability, low surface tension (cause of hydrophobicity), low dielectric constant, excellent electrical insulating properties (due to its low relative permittivity of 2.0-2.2), low flammability, low friction coefficient and high breakdown strength (19.2 kV/mm).[11, 12, 27-29]

As a result fluorocarbon coating find applications pharmaceutical industries for controlled drug release, insulation in aerospace industry, hydrophobic coatings on windshield etc.[12] The fluorocarbon functionalization with plasma system on CNT ribbons will enable coating of Teflon by other techniques.

1.5. Overview of functionalization of fluorine from literature review

Margrave et al have fluorinated SWNT in the temperature range of 150 – 500 °C by fluorine compounds.[30] However, the ends and/or sidewalls of CNT can be damaged during the process.[31] Plank et al functionalized CNT by plasma using CF_4 as the precursor, but the highest F/C ratio observed in their samples was 0.22, which is less than expected value of 0.5.[32] Abadjieva et al deposited fluorocarbon coatings on micron-sized silica particles with octafluorocyclobutane (C_4F_8), hexafluoropropylene (C_3F_6), trifluorethanol ($C_2H_3OF_3$) and hexafluoro-2-propanol ($C_3H_2OF_6$) using dielectric barrier discharge. However they observed that the coatings were flaky.[12] Kumar et al have used 1H,1H,2H,2H-perfluorodecyl Acrylate-1 for functionalization of silicon wafers. Although their coatings indicated F/C ratio of 1.08 – 1.21, their process if confined to low pressure plasma system.[29]

1.6. Applicability of plasma for functionalization of CNT ribbons with fluorine

In the last few years, plasma polymerization on the surface of CNT has become a preferred method for functionalizing surfaces.[31, 33] Plasma polymerization refers to “the formation of polymeric materials under the influence of plasma”.[34] The films formed by plasma system are ultra-thin, chemically inert and they adhere strongly to various

substances like polymers, metals, ceramics etc.[35] Its advantages over electrochemical or chemical techniques are:[32-34, 36, 37]

(i) Solvent free process,

(ii) Polymeric films that do not produce through normal chemical routes can produced by plasma polymerization,

(iii) Strong adhesion to substrate,

(iv) Generates no waste disposal, and

(v) Coating process takes at room temperature.

Plasma polymerized films can be used for several applications, such as: anti-corrosive coatings, humidity sensors, scratch resistance coatings, protective coating, and hydrophobic or hydrophilic coating.[37]

1.7. Conclusions from literature survey

Literature survey shows that greater number of papers have been published on plasma polymerization of fluorocarbon monomers using low pressure plasma system as compared to atmospheric pressure plasma system.[12] In addition, to the best of our knowledge no reported efforts in literature relate to the use of perfluoroheptane and perfluoro(methylcyclohexane) for functionalization of carbon nanotube ribbons using atmospheric pressure microwave plasma system.

With an intention of advancing the research in plasma functionalization of CNT materials, this research deals with the application of atmospheric pressure microwave plasma system for functionalization of fluorocarbon compounds.

2. Objectives of thesis

A. Reengineer atmospheric pressure microwave plasma for efficiently functionalization of CNT materials.

B. Functionalize CNT ribbons with different fluorocarbon monomers.

C. Characterize the film formed on CNT ribbons.

D. Explore possible application of functionalized CNT materials.

3. Experiments

3.1. Materials used

All the gases used for the experiments were purchased from Wright Brothers, Inc. (Cincinnati, OH). He-H_2 (gas mixture), He, Ar, H_2, C_2H_4 had a purity of 99.999%. Perfluoroheptane (mixed isomers, 98% purity; PFH), 1H,1H,2H,2H-Perfluorodecyl acrylate (96% purity; PDA) and Perfluoro(methylcyclohexane), (94% purity; PFMCH) were the monomers used for thin film deposition experiments. All the monomers were purchased from Alfa Aesar, USA.

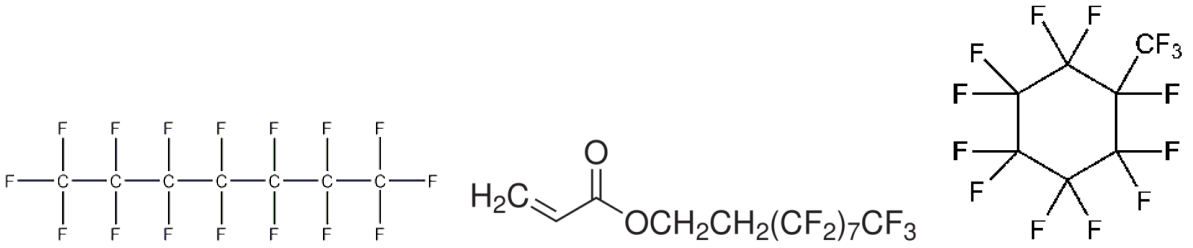

Figure 6 Chemical structures of PFH, PFDA and PFMCH.

Perfluoroheptane has suitable deposition rate and ability to form good cross linked hydrophobic layer [29].

Considering the ease of availability of and cost of lint free paper in comparison to CNT ribbons, lint free papers were used to determine the optimum coating conditions. Conditions which resulted in hydrophobic transparent films were repeated for coating CNT ribbons.

3.2. Synthesis of CNT array and drawing CNT ribbons

Spinnable carbon nanotubes (CNT) were synthesized by chemical vapor deposition (CVD) in a reactor manufactured by First Nano (CVD Equipment Corp.). Ethylene was cracked in the presence of Ar, H_2 and water vapor in the reactor. CNT were grown at 750°C on silicon substrates pre-coated with Fe based catalyst. CNT were pulled from one end of the CNT array and wound on a PTFE belt several times. CNT yarn was obtained by twisting the ribbon as it was being pulled from the CNT array [38, 39].

Figure 7 (a) shows CNT ribbon being spun from CNT arrays and figure 1 (b) is the SEM image of the ribbon at 1000X.

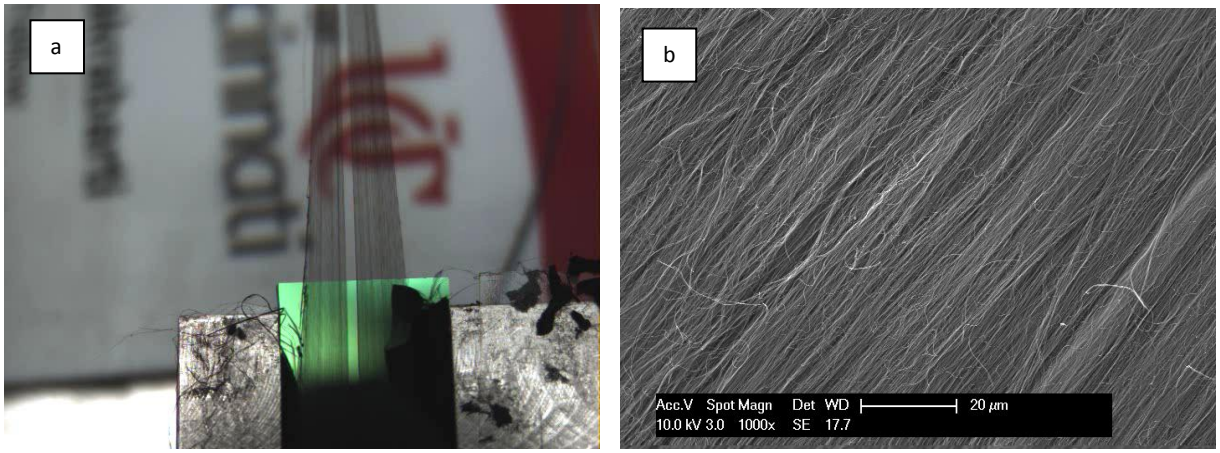

Figure 7 CNT ribbon. (a) ribbon being spun from spinnable CNT arrays at UC Nanoworld, (b) shows uncoated CNT ribbon as observed in SEM at 1000X magnification.

3.3. Functionalization of CNT ribbons

The CNT ribbons were coated by 1500 W atmospheric pressure microwave plasma system, manufactured by ASTEX Corporation (a subsidiary of MKS Instruments, Inc.). Figure 8 shows the schematic of the setup used for functionalization experiments.

As the plasma gas flows through the quartz torch (Figure 9), it interacts with microwaves in the presence of a ceramic rod to generate plasma.[13] The plasma gas used for the synthesis of thin films used a mixture of 99% He + 1% Hydrogen or only He. The flow rate of plasma gas varied from 2 Lpm to 5 Lpm.

He was used the monomer carrier gas and its flow rate varied from 0.8 Lpm to 1.4 Lpm. The vapors of the monomer pass through a flexible pipe to inner jacket of the quartz torch through an inlet tube attached to quartz torch. The architecture of quartz torch causes monomer vapors to be broken down into radicals on interacting with plasma species. The monomer radicals flow downwards along with the stream of plasma gas and settle on the substrate, where they polymerize.

Table 1 summarizes some of the key plasma functionalization experiments on Si wafer, tissue paper, cloth, graphite, CNT ribbon and thread.

3.4. Pulsing APMP

In order to further decrease the surface energy at the air-solid surface of the functionalized samples, the extent of fluorination of carbon atoms has to be increased

by operating the plasma system in pulsed mode.[40] During the pulsing mode, the frequency and power of the plasma system were controlled by an external function / arbitrary waveform generator from Agilent Technologies (model no: 33220A). As per ASTEX's design of the microwave plasma system, 1 V of external voltage corresponds to 150 W and 10 V corresponds to 1500 W of microwave power. Figure 10 represents the circuit diagram for using plasma system in pulsing mode. Some of the process parameters used for the pulsing experiments have been mentioned in Table 2.

However the XPS and TOF SIMS characterization results were not satisfactory, so they have not been included in the thesis.

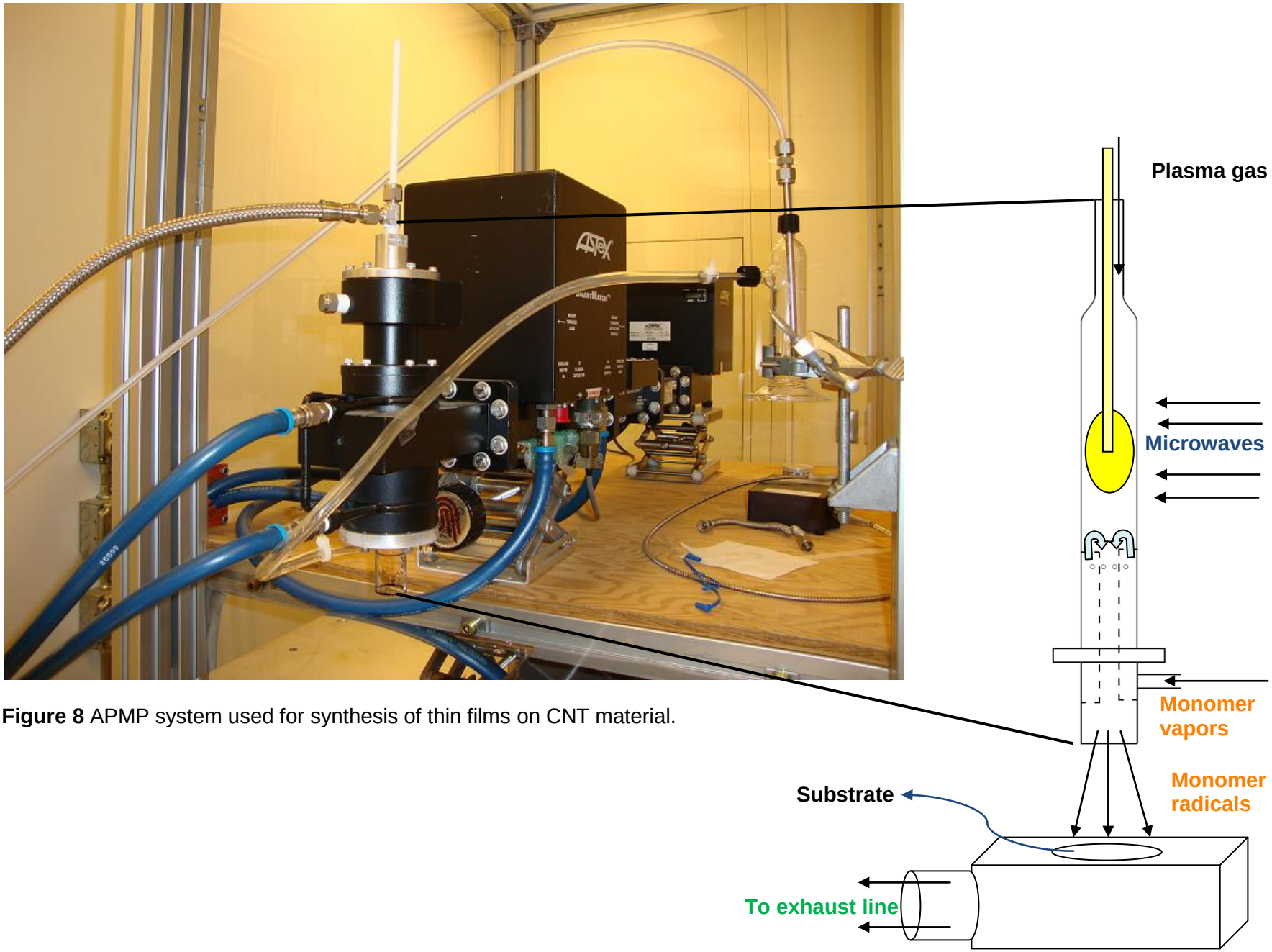

Figure 8 APMP system used for synthesis of thin films on CNT material.

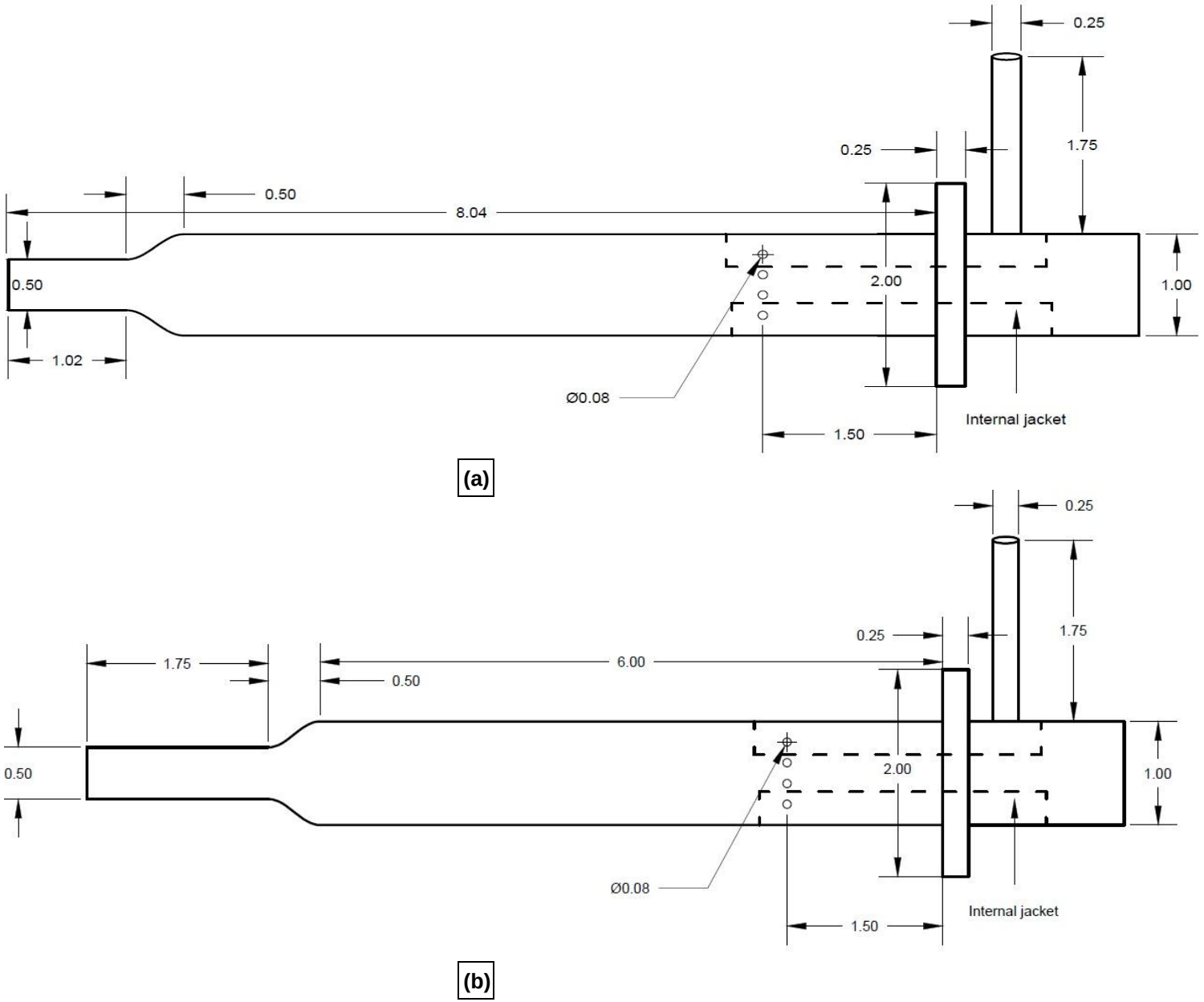

Figure 9 Quartz torches used for coating of CNT ribbons, (a) improved design, (b) original design. *(All dimensions are in inches.)*

Table 1 Summary of key plasma functionalization experiments on Si wafer, tissue paper, cloth, CNT ribbon and thread.

Sample ID	Coating conditions							Substrate	Visual Observations
	Power level (W)	Plasma gas	Plasma gas flowrate (lpm)	Monomer carrier gas	Monomer carrier gas flowrate (lpm)	Monomer	Duration (min)		
1	180	He	3	He	1	PFH	1	Si wafer	Surface remains hydrophilic
2	150	He + H_2	5	He	1	PFH	1	Si wafer	Surface remains hydrophilic
3	150	He + H_2	6	He	1	PFH	3	Si wafer	Surface remains hydrophilic
4	150	He + H_2	8	He	0.8	PFH	1	Si wafer	Surface remains hydrophilic
4’	150	He + H_2	8	He	0.8	PFH	1	Graphite	Surface remains hydrophilic
5	150	He + H_2	10	He	0.8	PFH	1	Si wafer	Surface remains hydrophilic
5’	150	He + H_2	10	He	0.8	PFH	1	Graphite	Surface remains hydrophilic
6	190	He + H_2	4	He	1.4	PFDA	10	Tissue Paper	Surface remains hydrophilic
7	170	He + H_2	6	He	1	PFDA	15	Cloth	Surface remains hydrophilic
8	300	He	3	He	1	PFMCH	5	Tissue Paper	Paper oxidizes
9	300	He	5	He	1	PFMCH	10	Tissue Paper	Paper oxidizes
4K	170	He	3	He	1	PFH	2	Tissue paper	Surface turns hydrophobic
10	180	He	3	He	1	PFH	3	CNT thread	Thread becomes fragile. May be functionalized
2K	170	He-H_2	3	He	1	PFH	2	Tissue paper	Surface turns hydrophobic
5K	170	He	4	He	1	PFH	2	Tissue paper	Surface turns hydrophobic
2C	170	He-H_2	3	He	1	PFH	2	CNT ribbon	N/A
4C	170	He	3	He	1	PFH	2	CNT ribbon	N/A
5C	170	He	4	He	1	PFH	2	CNT ribbon	N/A
8K	170	He	3	He	1	PFMCH	2	Tissue paper	Surface turns hydrophobic
8C	170	He	3	He	1	PFMCH	2	CNT ribbon	N/A
TEF				Untreated				PTFE tape	N/A
CNT				Untreated				CNT ribbon	N/A

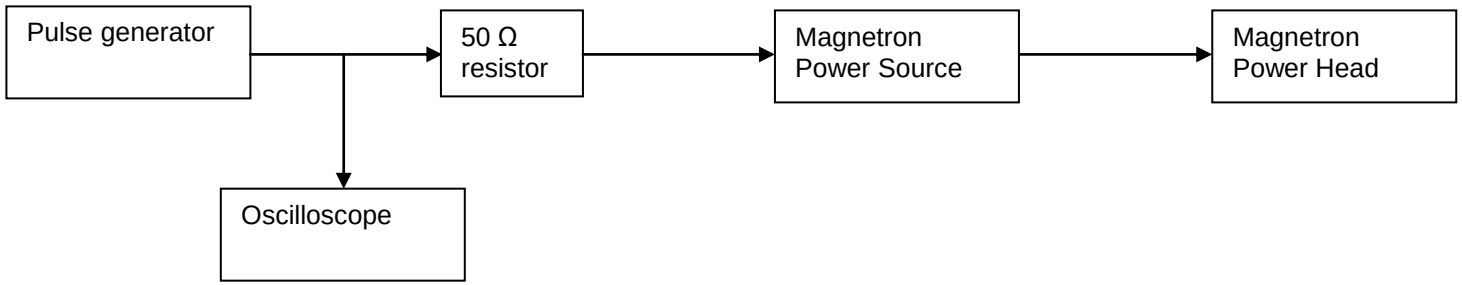

Figure 10 Circuit diagram for using plasma system in pulsing mode.

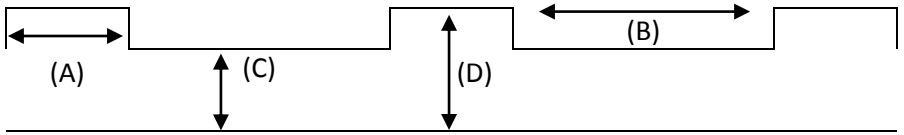

Figure 11 Waveform representing the operating conditions of plasma system. A: ON cycle time, B: OFF cycle time, C: Power level of magnetron during OFF mode, and D: Power level of magnetron during ON mode.

Table 2 Summary of key plasma functionalization experiments using pulsing mode.

Sample ID	Plasma gas	Plasma gas flowrate (lpm)	Monomer carrier gas	Monomer carrier gas flowrate (lpm)	Monomer	Substrate	Operating conditions				Duration (mins)	Visual Observations
							A (ms)	B (ms)	C (W)	D (W)		
1’	He	2	He	1	PFMCH	Tissue Paper	310	690	214	137	8	Surface remains hydrophilic
2’	He	4.2	He	1	PFMCH	Tissue Paper	310	690	214	137	10	Surface remains hydrophilic

3.5. Characterization of Samples

The composition of deposited films on CNT ribbons and tissue papers were analyzed by TOF-SIMS and XPS.

TOF-SIMS (ION-TOF) spectrometer used a pulsed Ga ion source (operating at 25kV) as the primary ion source. The secondary ions were extracted perpendicular to the sample surface at ± 2 kV (depending on the mode) and scanned 500 X 500 μm^2 area per sample. Peak assignment was done using SurfaceLab 6 (ION-TOF) software.

XPS was done using Phi (5300) and Surface Science Instruments (SSX – 1100). Phi(5300) used Mg Kα source, while SSX 1100 used monochromated Al Kα source. The characterization results of the CNT and paper samples have been described in the

CNT ribbons were observed under an environmental scanning electron microscope (Philips XL-30 FEG).

4. Results and Discussions

The fluorocarbon films were transparent and are expected to be hydrophobic in nature.[41] The presence of thin film was visually confirmed by observing whether a drop of water gets absorbed on the surface of tissue paper. Figure 12 shows a tissue paper sample functionalized by fluorocarbon films. The functionalized region on the tissue paper is hydrophobic, while the rest of the area is hydrophilic.

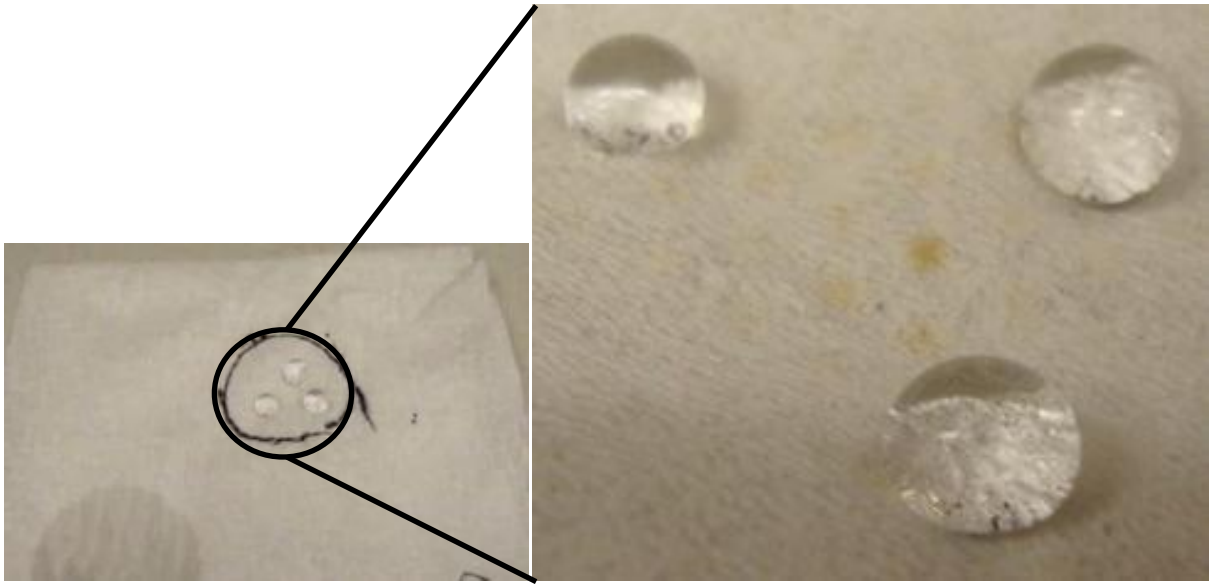

Figure 12 Drops of water on a region of tissue paper functionalized with fluorocarbon film (demarcated by black circle). The bottom left corner of the paper is uncoated and hence it absorbs water.

4.1. Time-of-Flight Secondary Ion Mass Spectrometry (TOF-SIMS)

TOF-SIMS characterizations were performed in order to analyze the backbone of deposited fluorocarbon film. Figure 13 - Figure 16 shows the TOF SIMS spectra of CNT and paper samples functionalized by using PFH as the monomer.

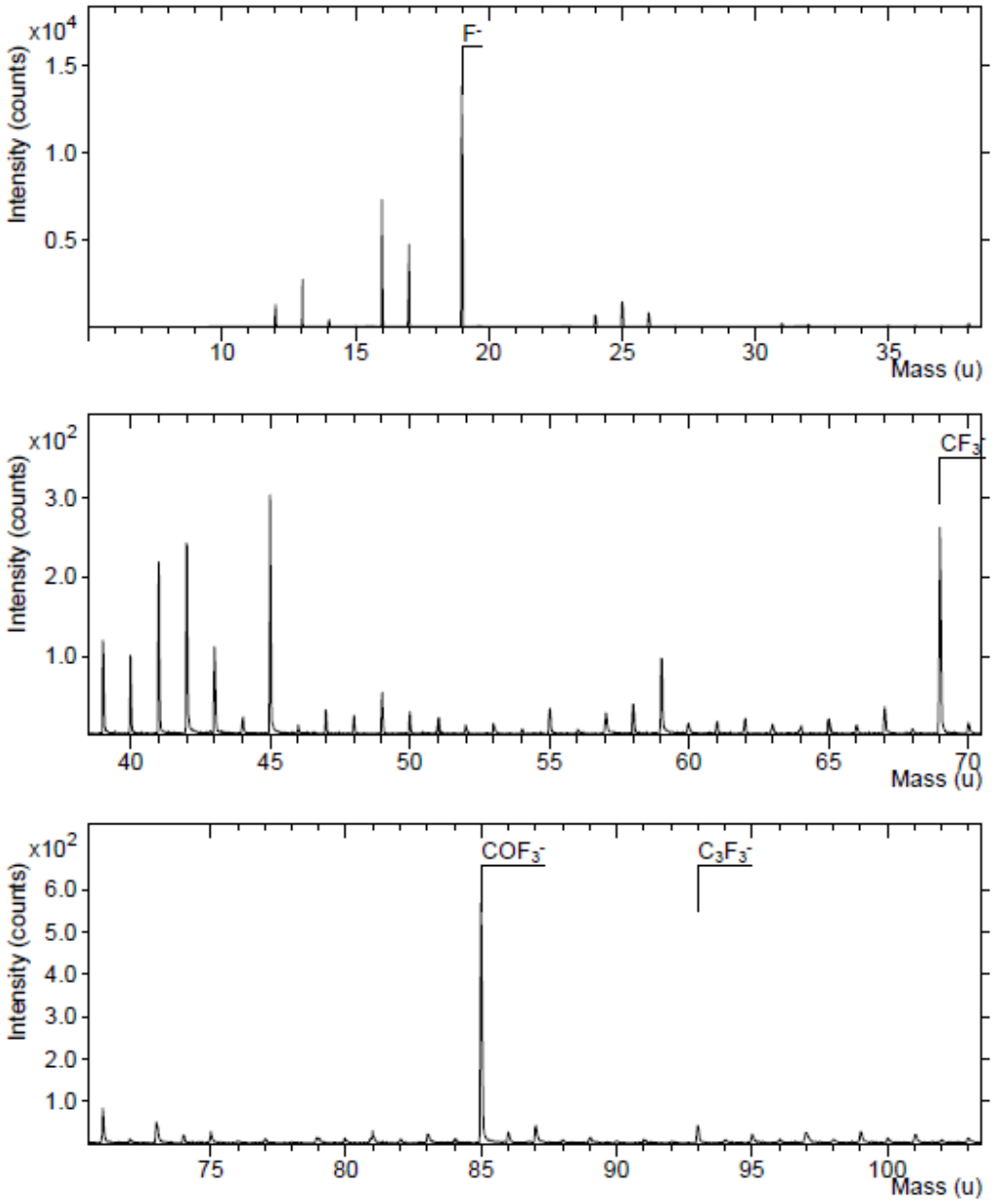

Figure 13 Negative TOF SIMS spectra of sample 2K.

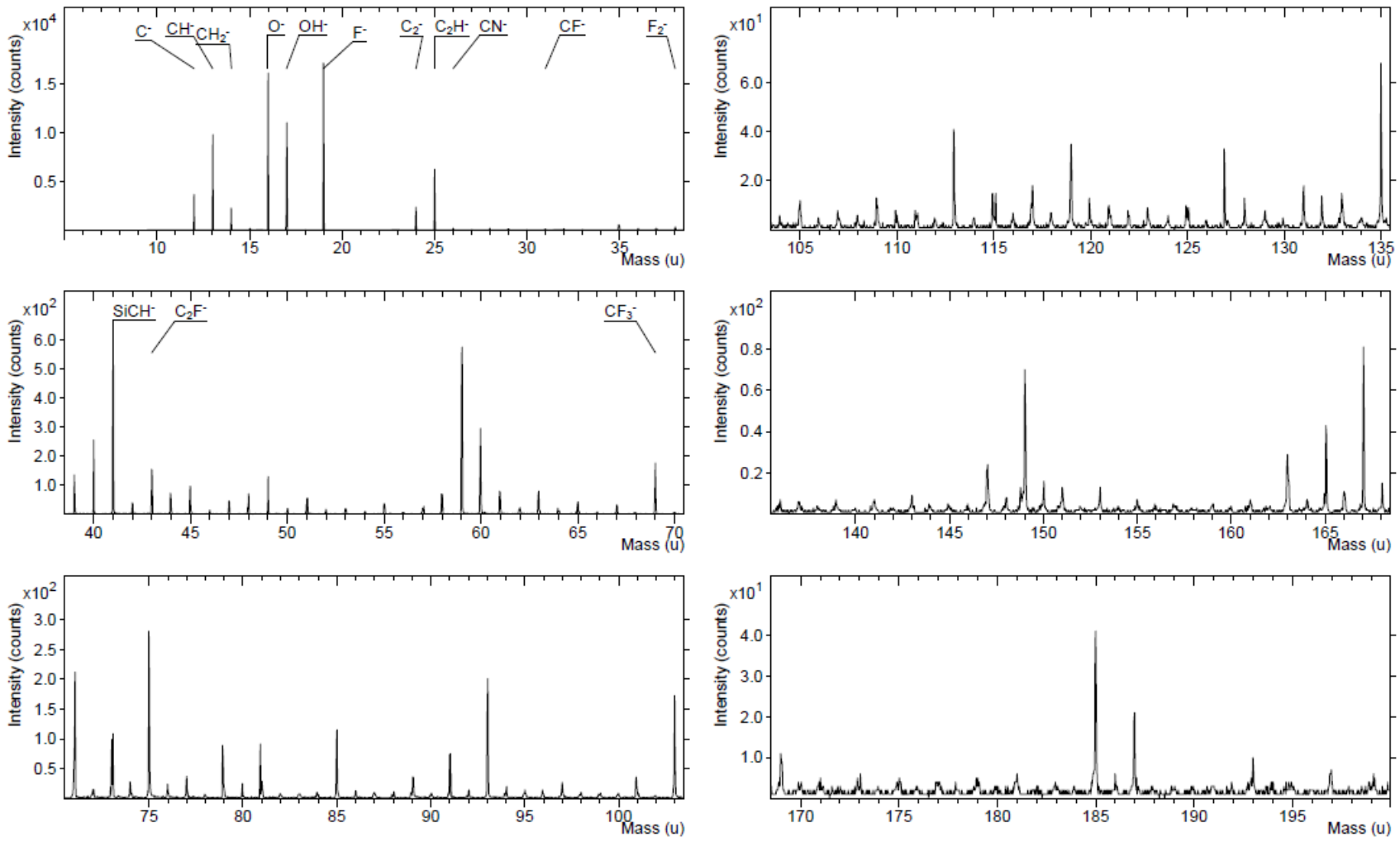

Figure 14 Negative TOF SIMS spectra of sample 2C.

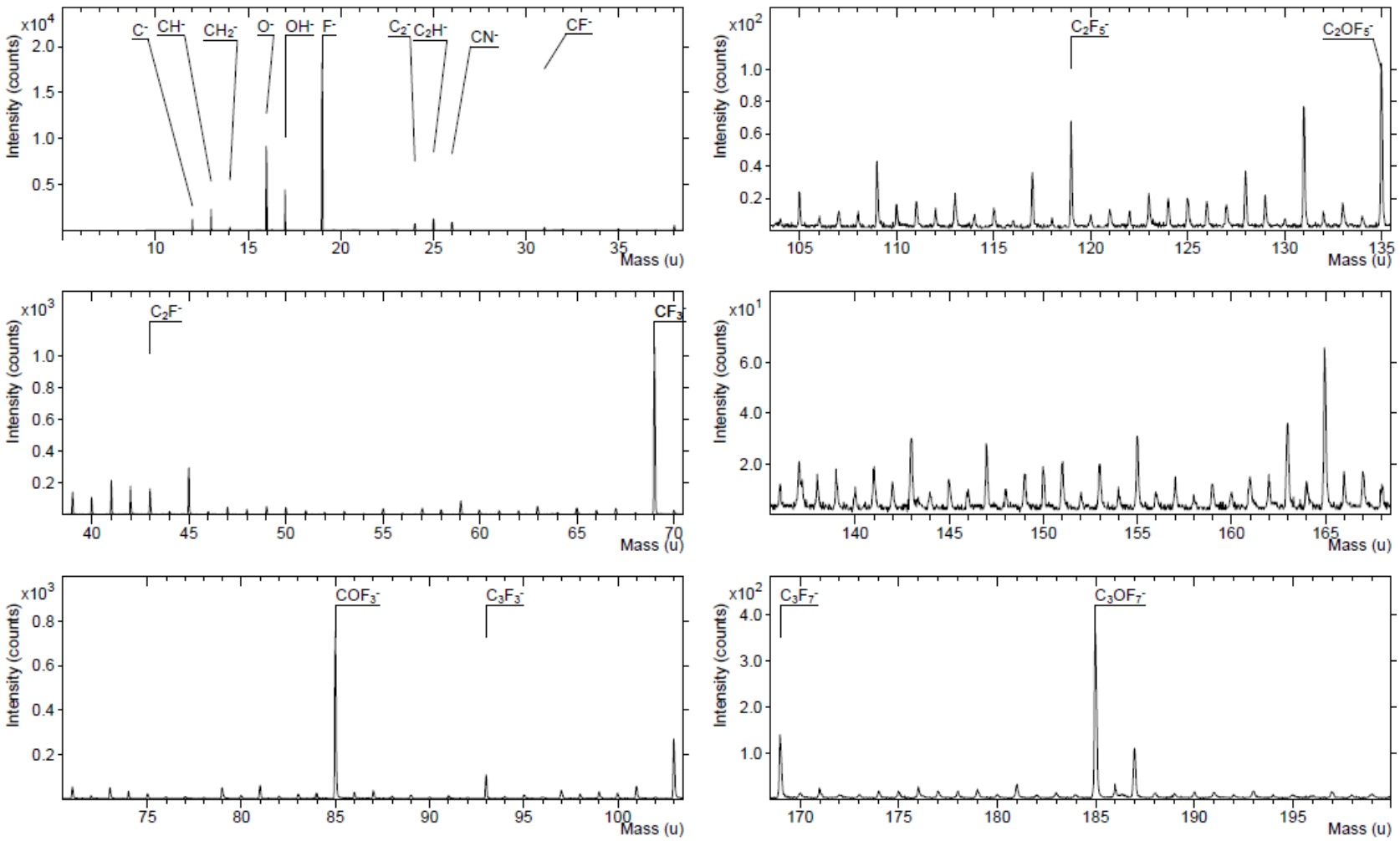

Figure 15 Negative TOF SIMS spectra of sample 4K.

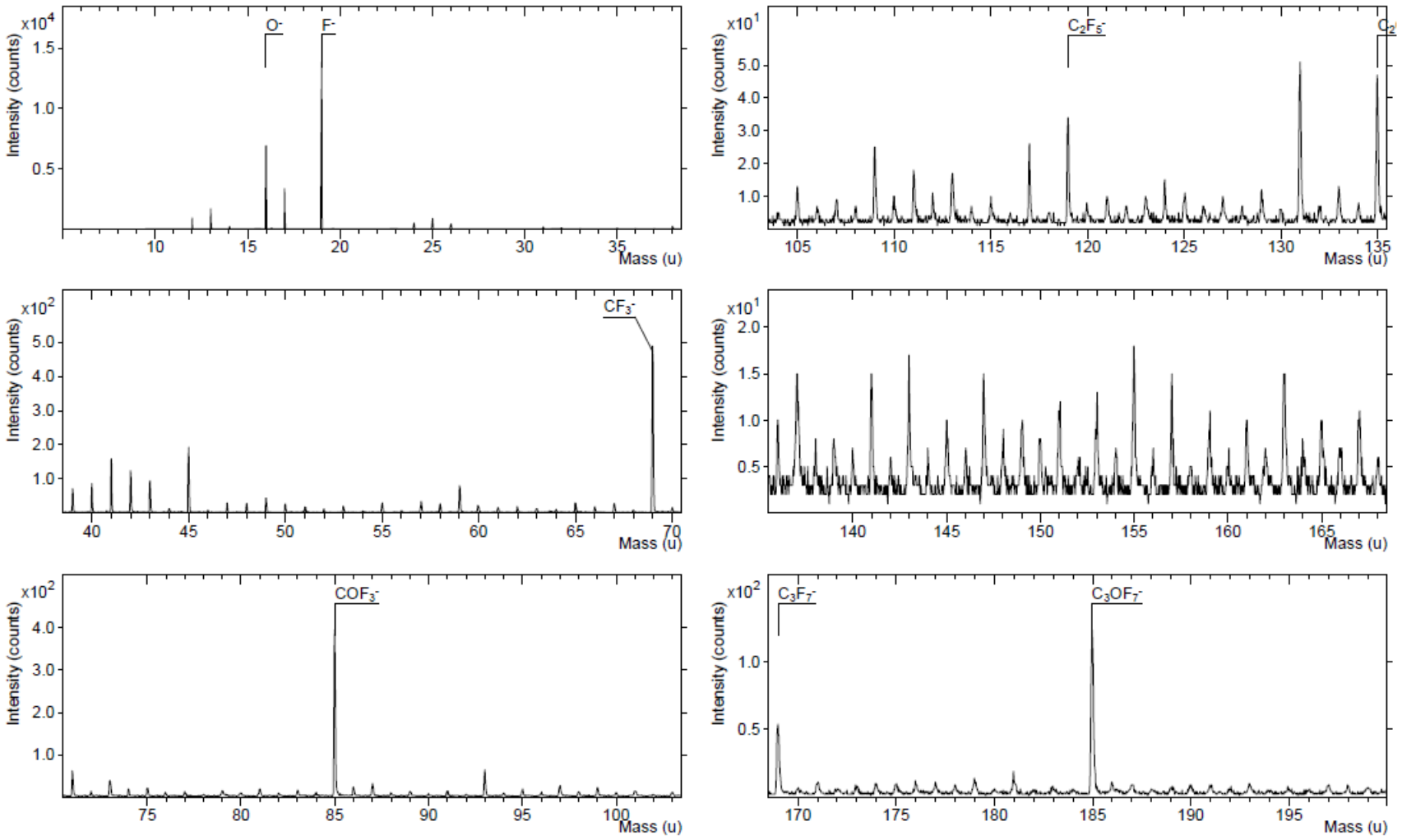

Figure 16 Negative TOF SIMS spectra of sample 5K.

Table 3 shows that the paper samples have a peak at m/z ratios of 16D and 17D, which correspond to O^- and OH^-. Peaks at m/z ratios of 19D, 69D, 93D, 119D, 169D and 193D are common to the TOF SIMS data of paper, CNT ribbons and polytetrafluoroethylene (PTFE; control sample). This analysis indicates that CNT and paper samples were functionalized with fluorocarbon compounds.

Table 3 Summary of peaks observed in TOF results of various samples.

m/Z (D)	Peak Assignment	Samples				
		2K	2C	4K	5K	TEF
16	O_2^-	Y	Y	Y	Y	
17	OH^-	Y	Y	Y	Y	
19	F^-	Y	Y	Y	Y	Y
43	C_2F^-	Y	Y	Y	Y	
69	CF_3^-	Y	Y	Y	Y	Y
85	COF_3^-	Y	Y	Y	Y	
93	$C_3F_3^-$	Y	Y	Y	Y	Y
119	$C_2F_5^-$	Y	Y	Y	Y	Y
169	$C_3F_7^-$	Y	Y	Y	Y	Y
193	$C_5F_7^-$	Y	Y	Y	Y	Y
251	$C_4O_2F_9^-$		Y			
301	$C_5O_2F_{11}^-$		Y			
351	$C_6O_2F_{13}^-$		Y			
417	$C_7O_3F_{15}^-$		Y			
467	$C_8O_3F_{17}^-$		Y			
517	$C_9O_3F_{19}^-$		Y			
583	$C_{10}O_4F_{21}^-$		Y			
633	$C_{11}O_4F_{23}^-$		Y			
683	$C_{12}O_4F_{25}^-$		Y			
699	$C_{12}O_5F_{25}^-$		Y			
749	$C_{13}O_5F_{27}^-$		Y			
799	$C_{14}O_5F_{29}^-$		Y			
849	$C_{15}O_5F_{31}^-$		Y			

In addition to the above mentioned peaks, sample 2C also shows the presence of peaks greater than 193D because the conductive nature of CNT ribbons provides an ideal electron source to the thin fluorocarbon film.

Closer examination of TOF-SIMS data (refer to Table 4 and Table 5) of functionalized paper samples and CNT ribbons reveals that there is a difference of 50D between various data points indicating that CF_2 is the repeating unit. Similar observations were made by Kinmond et al. when they characterized plasma polymerized samples using 1H,1H,2H-perfluorododecene as the precursor.[40]

Table 4 Selected data points of paper samples showing that the fragments are separated by m/z ratio of 50D.

m/z (D)	**Ions**	**$(m/z)_{i+1} - (m/z)_i$**
19	F^-	
69	CF_3^-	50
119	$C_2F_5^-$	50
169	$C_3F_7^-$	50

Table 5 Selected data points of sample 2C showing that the fragments are separated by m/z ratio of 50D.

m/z (D)	**Ions**	**$(m/z)_{i+1} - (m/z)_i$**	**m/z (D)**	**Ions**	**$(m/z)_{i+1} - (m/z)_i$**
251	$C_4O_2F_9^-$		583	$C_{10}O_4F_{21}^-$	
301	$C_5O_2F_{11}^-$	50	633	$C_{11}O_4F_{23}^-$	50
351	$C_6O_2F_{13}^-$	50	683	$C_{12}O_4F_{25}^-$	50
417	$C_7O_3F_{15}^-$		699	$C_{12}O_5F_{25}^-$	
467	$C_8O_3F_{17}^-$	50	749	$C_{13}O_5F_{27}^-$	50
517	$C_9O_3F_{19}^-$	50	799	$C_{14}O_5F_{29}^-$	50
			849	$C_{15}O_5F_{31}^-$	50

Strong peaks are observed between 417D and 849D, which suggests that fragments contain more carbon atoms than the monomer (perfluoroheptane). Thus it can be concluded that radicals have polymerized on the surface of CNT ribbon.

4.2. X-ray Photoelectron Spectroscopy (XPS)

In XPS, the X-rays penetrate through the surface of the sample up to ~ 50 Å, causing the electrons to eject from its surface. The number of electrons and their energy gives a measure of the relative elemental concentration on the surface of the sample. The energy of the ejected electrons is also a factor of the electronegativity of the nearby atoms.[42] Thus curve fitting the peaks obtained by high resolution scan can give an indication of the functional groups present in the coating.

Literature review shows that XPS is a popular technique for characterization of fluorinated samples.[42] Therefore XPS has been extensively used for characterization of functionalized samples.

The results obtained by scanning sample are shown in Figure 17 - Figure 24.

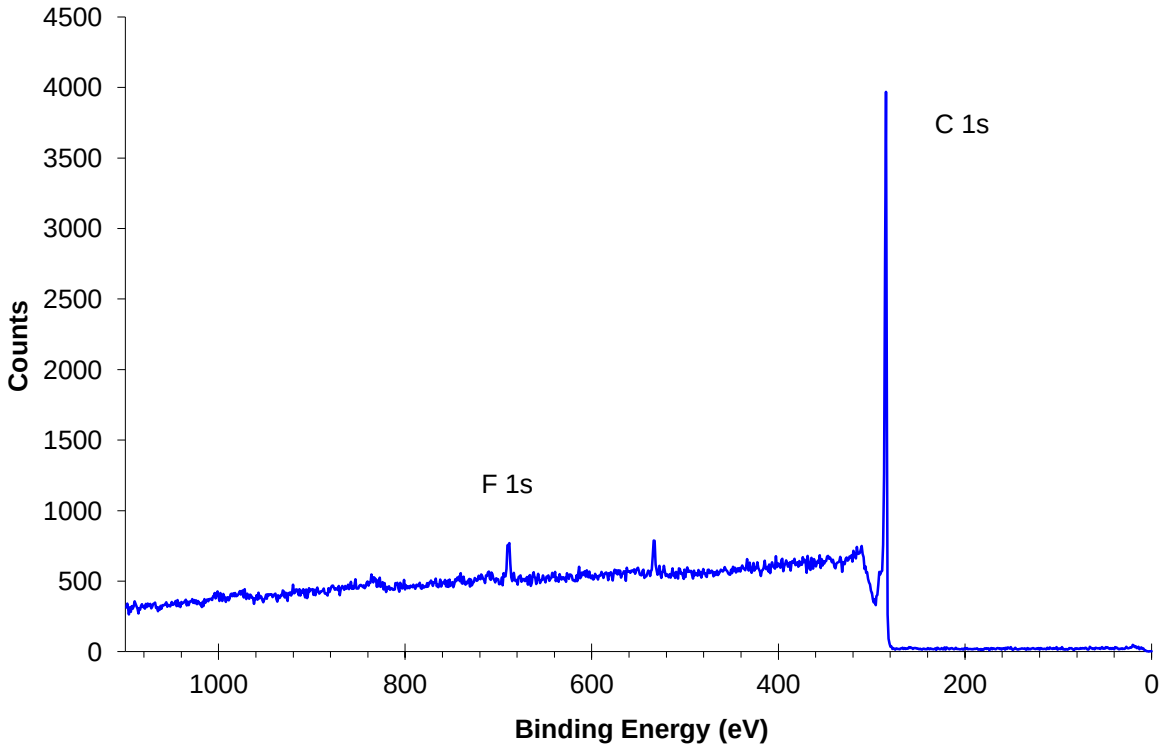

Figure 17 Survey scan of sample 2C using XPS.

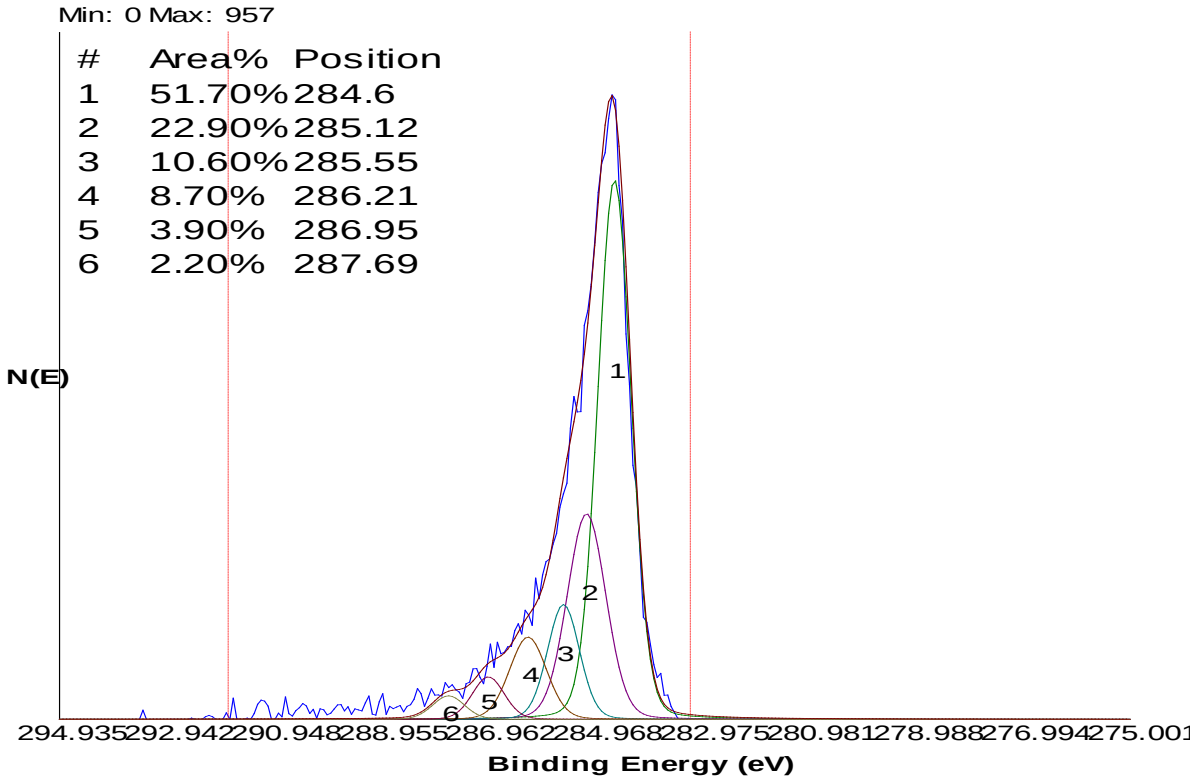

Figure 18 High resolution scan of sample 2C using XPS.

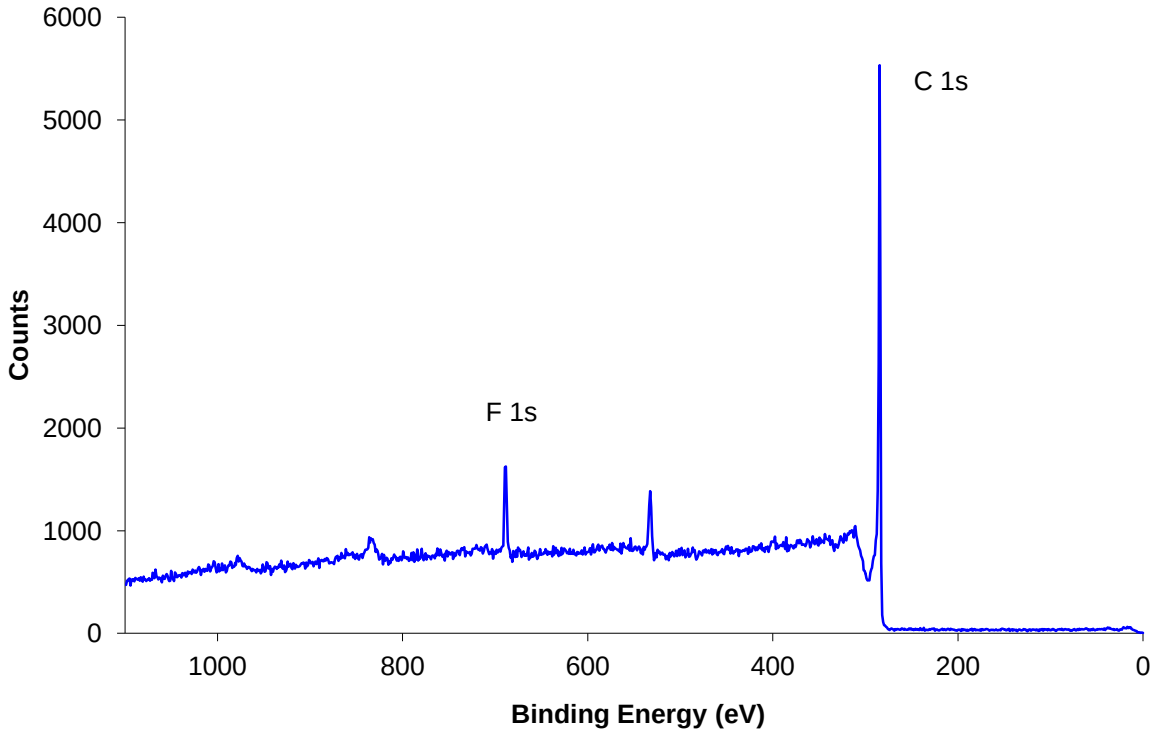

Figure 19 Survey Scan of Sample 4C using XPS.

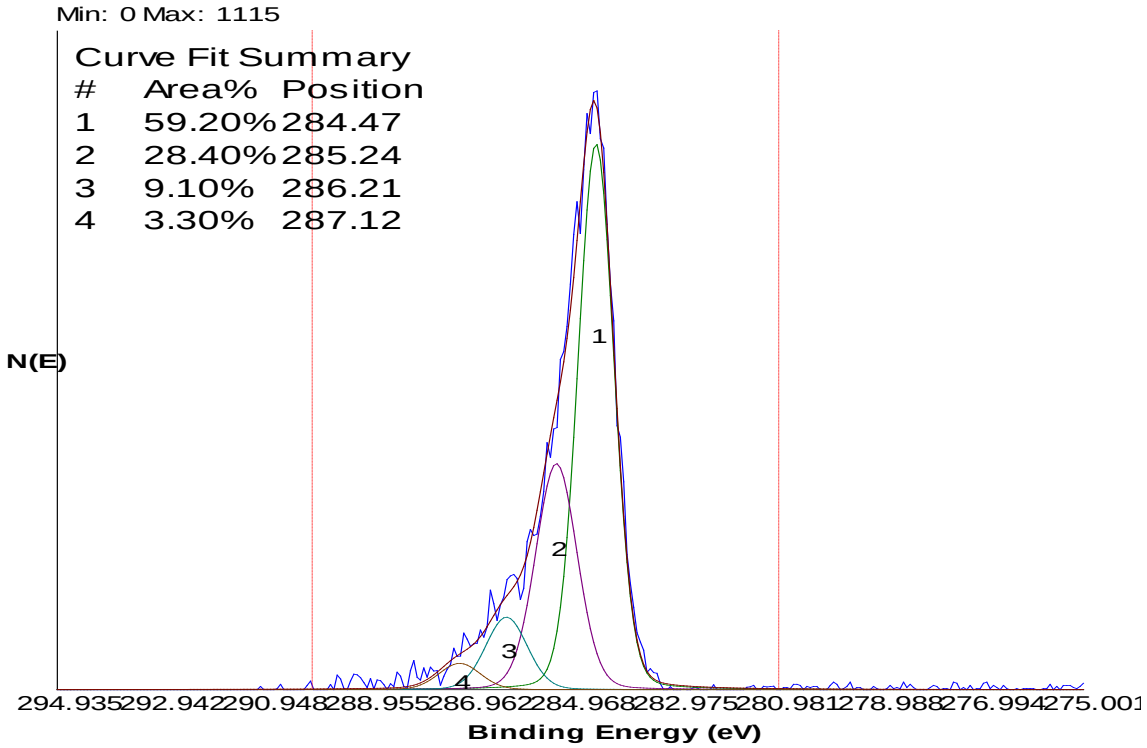

Figure 20 High resolution scan of sample 4C using XPS.

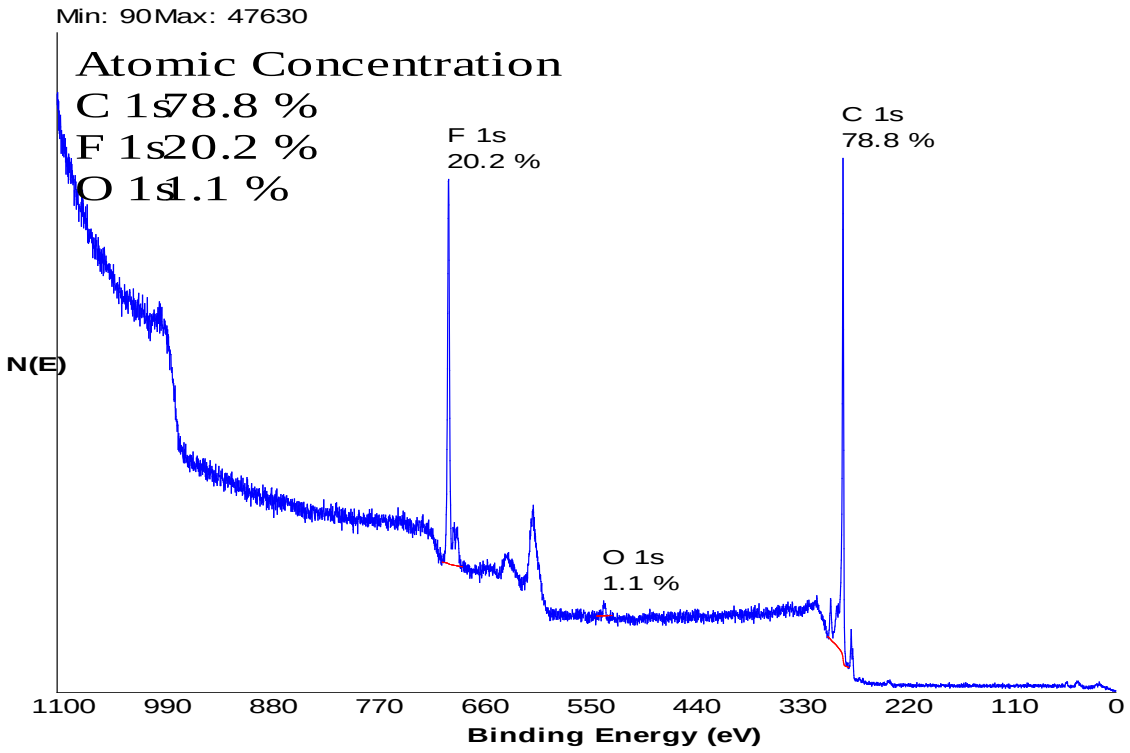

Figure 21 Survey scan of sample 5C using XPS.

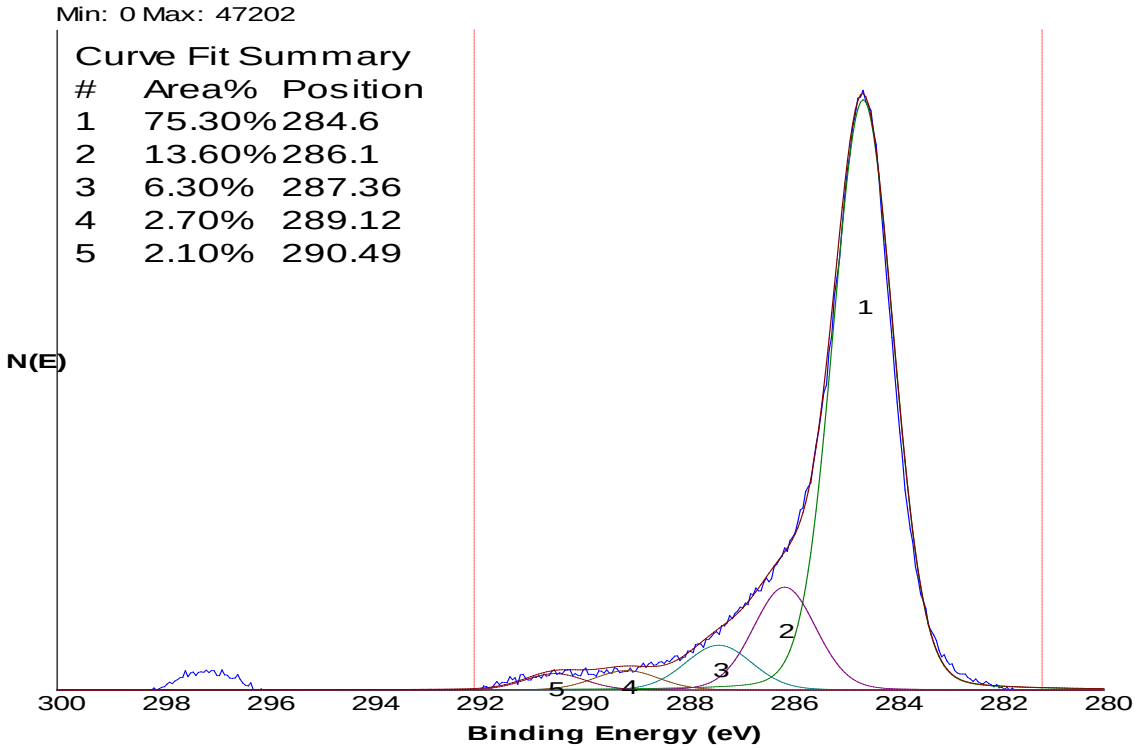

Figure 22 High resolution scan of sample 5C using XPS.

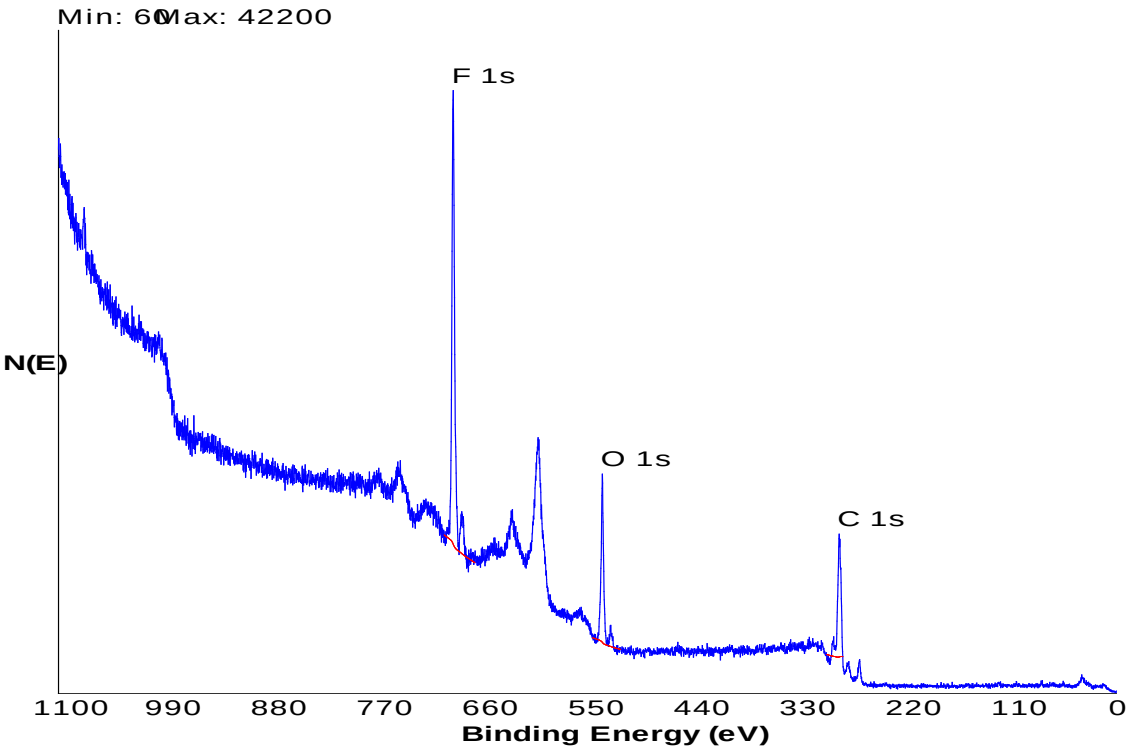

Figure 23 Survey scan of sample 8K using XPS.

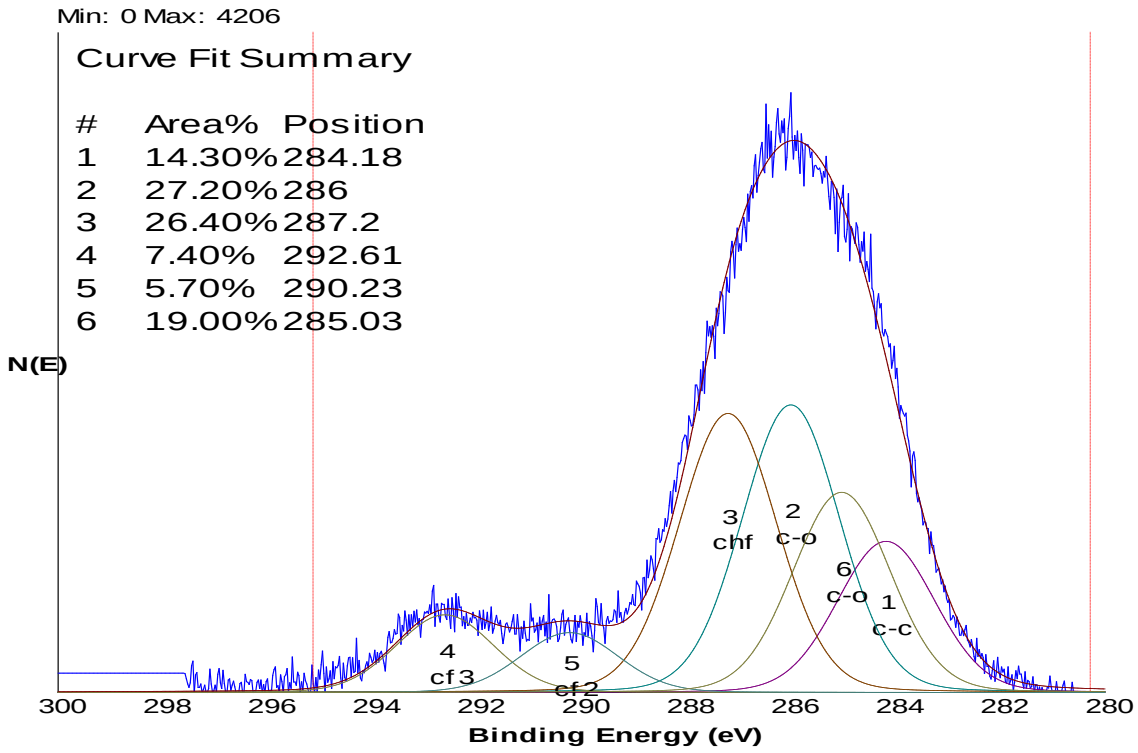

Figure 24 High resolution scan of sample 8K using XPS.

Table 6 and

Table **7** summarize the XPS data obtained for selected samples.

Table 6 Average elemental compositions of selected samples obtained by XPS.

Sample ID → / **Elemental concentration (%)** ↓	**4K**	**5K**	**2C**	**4C**	**5C**	**8K**	**8C**	**TEF**	**CNT**
F	10.8	12.0	2.9	7.6	11.2	43.1	1.9	73.0	0.0
O	31.9	20.8	3.8	9.6	3.2	22.5	1.4	0.0	13.7
C	56.4	65.5	93.3	82.8	85.6	34.4	96.7	27.0	85.1

Table 7 Peak assignment and area under the fitted curves for CNT ribbon samples (2C, 4C) and paper sample (5K).

Peak	**Binding Energy (eV)**	**% area under the curve**				
		2C	**4C**	**5K**	**5C**	**8K**
C – C [43]	284.6	51.7	63.2	26.7	75.3	14.0
sp^2 C – C bonds [44]	285.12 - 285.55	33.5	0	0	0	0
C – O (in ether, alcohol) [43, 45]	286.04 - 286.95	12.6	13.5	41.8	13.6	46.5
– CF_x [28], –CHF [43]	287.12 – 290	2.2	20.4	29	9	26.4
– CF_2 [28]	291.15	0	2.9	0.9	2.1	5.7
– CF_3 [28, 43]	293.07	0	0	1.6	0	7.4
TOTAL		100	100	100	100	100

From Table 7 it can be inferred that coated paper samples have higher oxygen content than coated CNT ribbons, which could be due to oxygen contained in the cellulose of the paper (substrate) contributes to the XPS signal.

5. Conclusions

A. It has been demonstrated that atmospheric pressure microwave plasma system can be successfully employed for functionalization of tissue paper samples and CNT ribbons.

B. Fluorocarbon films were deposited on paper samples and CNT ribbons.

C. Fragments observed in TOF SIMS contained more carbon atoms than the monomer, indicating that radicals have polymerized on the surface of CNT ribbons. Also, a fragmentation pattern of $C_nO_xF_{2n+1}$ has been observed from the TOF SIMS data.

D. XPS data suggests that He is a better plasma gas as compared to He + 1% H_2 because of the reactions that may occur between CF radicals and hydrogen gas atoms/ions.

E. Porous substrates had greater functionalization with fluorocarbon films as compared to non-porous counterparts. This is because porous substrates allow plasma effluent gases to pass though them without heating the substrate. Due to this reason, the temperature of Si and graphite substrates increased significantly during the experiment causing the fluorocarbon films to oxidize or to be hindered from getting adsorbed.

F. Due to the functionalization on the surface of CNT ribbons, they might have better bonding with the matrix material of the composites. This might give rise to stronger light weight composites.

Section 3: Application of Atmospheric Pressure Microwave Plasma for Disinfection of Water Contaminated by *Bacillus globigii* Spores

Abstract

APMP was examined as a disinfection technique for *Bacillus globigii* spores. When He-H_2 gas mixture and O_2 were used as plasma gases, the water sample was completely disinfected. Use of He-H_2 gas mixture produced intense UVC (280 – 100 nm), MUV (300 – 200 nm) and UVB (315 – 280 nm). UVC are highly energetic form of ultraviolet radiation and are known to have germicidal effects. On the other hand, metastable oxygen species produced by the plasma system can be the most probable cause of sterilization of *Bacillus globigii* spores.

The results show that APMP can effectively decontaminate water containing *Bacillus globigii* spores. Thus, AMPM may be a suitable alternative to conventional disinfection techniques (e.g. chlorination, UV) for disinfecting water contaminated by BWA.

1. Introduction

1.1. Susceptibility of water bodies to biological warfare attack

Access to pure drinking water is a basic necessity of life. In case of an attack on water bodies with BWA, life can be greatly endangered. *Bacillus anthracis* (which causes anthrax) is listed under Category A by Center of Diseases Control and Prevention, in other words this bacterium poses a great risk to national security.[46] Thus there is a need for developing water purification techniques that can decontaminate water with minimum use of chemicals and toxic substances.

1.2. Existing decontamination techniques and their limitations

"Wet" solutions for decontamination such as hypochlorite bleaches, Oxone® (DuPont product containing active ingredient of potassium peroxymonosulfate $KHSO_5$) and Decontamination Solution 2 (DS2) do not seem suitable for treating water due to the corrosive nature of these chemicals. Additionally, these substance require large storage volumes, are not environmentally friendly and their disposal is a major issue.[9, 47]

Alternatively, gamma (γ) rays from radioactive sources (like Co-60) can also be used for disinfecting water. In order to prevent the leak of radioactive material and radiation, the facility has to be properly shielded. [9, 48] Consequently, the portability of the disinfection system is very limited.

Literature review suggests that *Bacillus anthracis* contained in water can be inactivated by heating it to 95°C for 25 minutes.[49] However, this technique is not feasible for decontaminating water on a large scale.

Water can also be disinfected by UV radiation. However, UV is most effective when the wavelength of incident radiation is in the range of 220 – 280 nm [8] and specifically, 254 nm, where DNA adsorption is at its maximum.[50] As a result, the DNA of the spores get damaged beyond repair leading to death.[51]

The average intensity of radiation incident on 1 cm^2 of sample is determined by:

$$I_{avg} = \frac{I_0 [1 - \exp(-\alpha H)]}{\alpha H}$$

where,

I_{avg} = Average intensity of UV_{254} incident on sample

I_0 = UV_{254} from the source

$\alpha = \ln(T) / L$

T = transmittance of UV_{254} radiations on spore solution

L = optical path length for transmittance measurement

H = depth of aqueous spore solution

(UV transmittance is measured for λ = 254 nm and path length = 1 cm [52])

Therefore, increase in turbidity of water (due to sand or impurities) can severely affect the effective range of disinfection of UV radiation. Also, if the flow of water is rapid, the exposure to UV will not be sufficient.

1.3. Conclusions from literature review

There is a pressing need for developing an environmentally friendly water purification technique that can decontaminate drinking water polluted with BWA. Literature survey shows that plasma systems can produce UV radiation, reactive oxygen species (ROS), reactive nitrogen species (RNS), ozone, metastable oxygen species etc which have the capability of decontaminating biological warfare agents.[9, 48, 51, 53] In addition, the plasma effluents recombine to form non-reactive species very rapidly. Thus, they do not damage sensitive equipment or corrode metal.[9] In addition, plasma systems can be easily transported to the site that has to be decontaminated.[9]

Since *Bacillus anthracis* requires special handling precautions, *Bacillus globigii* were used for all the experiments. *B. globigii* belong to a class of microorganisms that are the hardest to sterilize and they are often used as surrogates of *Bacillus anthracis.*[9, 54]

2. Objectives

A. Customize atmospheric pressure microwave plasma system for disinfecting water contaminated by *Bacillus globigii* spores.

B. Evaluate the effectiveness of atmospheric pressure microwave plasma system for treatment of water contaminated by *B. globigii* spores.

C. Characterize the plasma generated and ascertain the cause(s) for disinfection of *B. globigii* spores.

3. Experiments

3.1. Materials used

B. globigii spores were obtained from the Dugway Proving Ground. Spore preparation was done according to the method previously described by Szabo, Nicholson and Setlow.[55, 56] The spores were then stored in 40% ethanol solution at 4°C for future use. *B. globigii* are classified as “Class 1” organism by The National Institutes of Health's Centers for Disease Control; meaning it is harmless and non-pathogenic to humans.

All the gases used for the experiments were purchased from Wright Brothers, Inc. (Cincinnati, OH). He + 1% H_2 (gas mixture), N_2, and He had a purity of 99.999%, whereas O2 had a purity of 99.98%.

Experiments were performed with HPLC grade water from Tedia. Samples were drawn from the beaker using a sterile polystyrene disposable serological pipette and transferred into a sterile vial, both from Fisher Scientific. The diluted samples were uniformly spread out on three Trypticase Soy Agar plates (TSA) from Remel (part of Thermo Fisher Scientific).

3.2. Observing B. globigii under Scanning Electron Microscope (SEM)

In order to prepare the sample for SEM, 0.1 mL of concentrated spore solution was diluted in 10 mL of HPLC grade water. The resulting solution was mixed homogenously before pipetting 0.1 mL. The pipetted solution was uniformly spread on ITO glass, which was then dried in an oven at 37°C for a few minutes. The sample was scanned using

SEM without any further preparation. Figure 25 shows SEM image of B. globigii at 10kX.

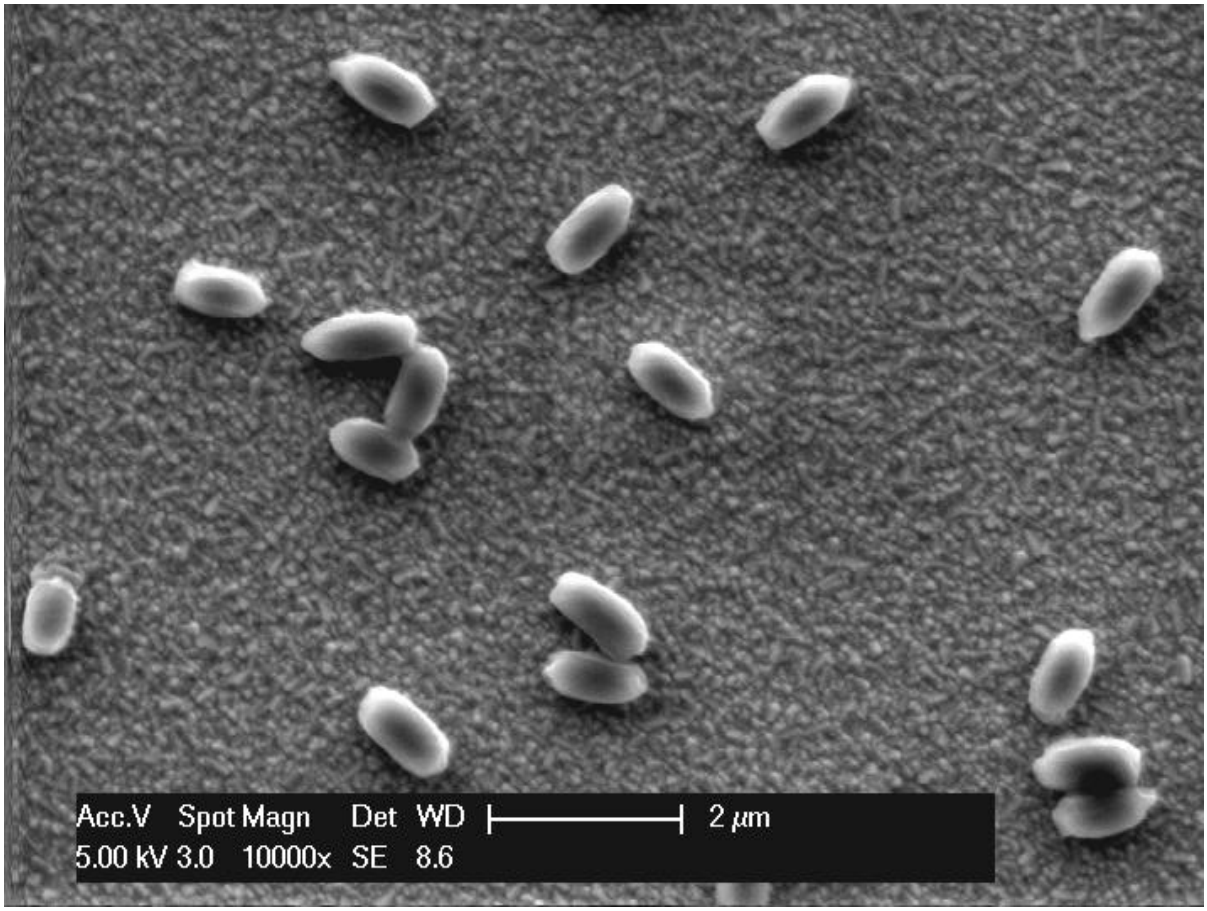

Figure 25 SEM image of *B. globigii* spores at 10k X.

3.3. Preparation of water sample contaminated by B. globigii

A homogenous solution of *B. globigii* was prepared by mixing 0.1 mL of concentrated spore solution with 350 mL of HPLC grade water. At time t = 0 min, 10 mL of sample was drawn from this beaker and transferred into a sterile vial.

3.4. Disinfection of water contaminated by B. globigii using plasma system

Plasma was fired with He, He–H_2 gas mixture, N_2 or O_2 and generator power was set to 250 W, 325 W or 400 W depending on the experiment. Based on trial runs, no disinfection takes place when the power level of the generator is below 250 W. On the other hand, the plasma system begins to heat up rapidly if the power is above 400 W. Figure 26 shows the atmospheric pressure microwave plasma system. Figure 27 shows the modified quartz torch used for the disinfection experiments.

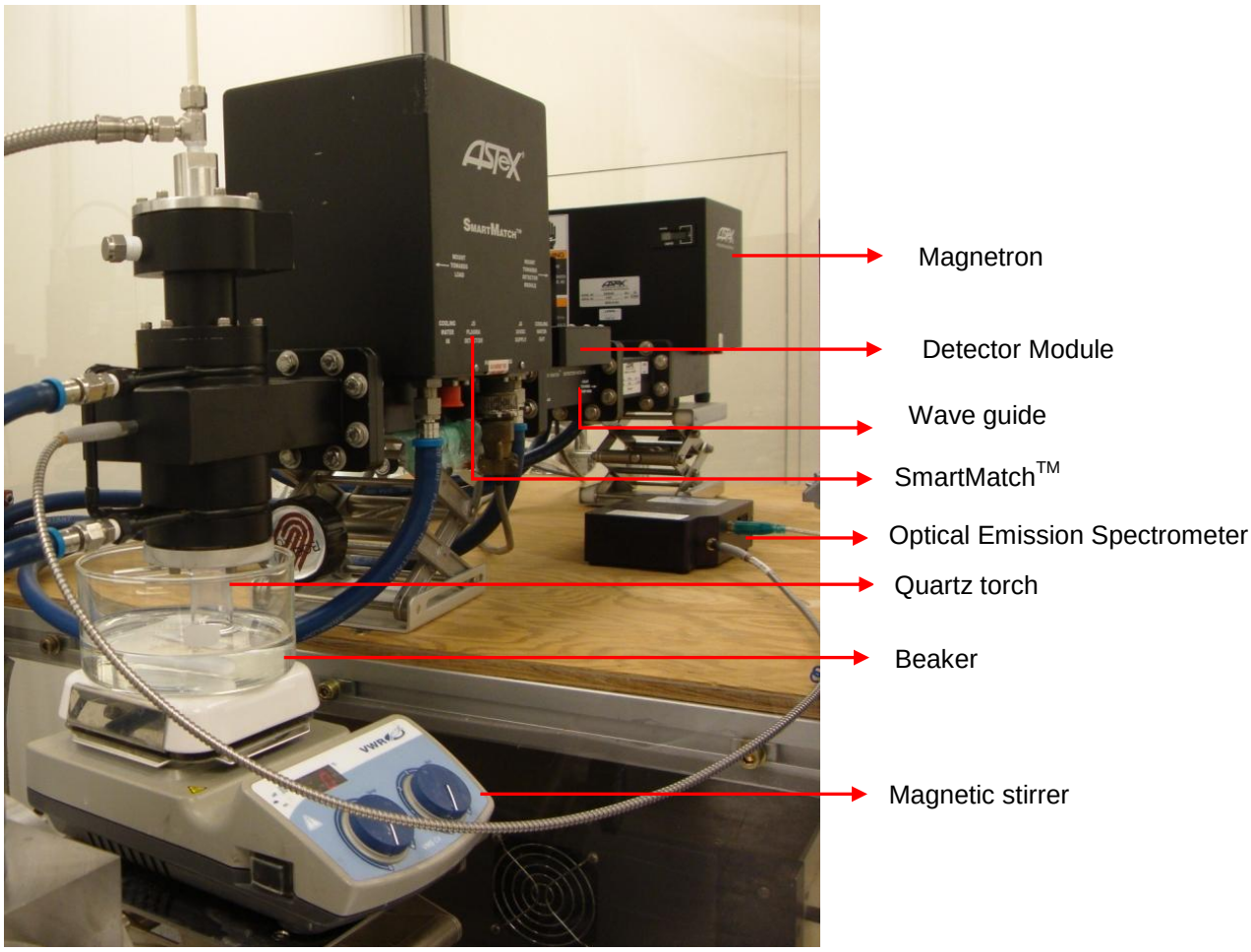

Figure 26 APMP used for disinfection of water contaminated by *B. globigii* spores.

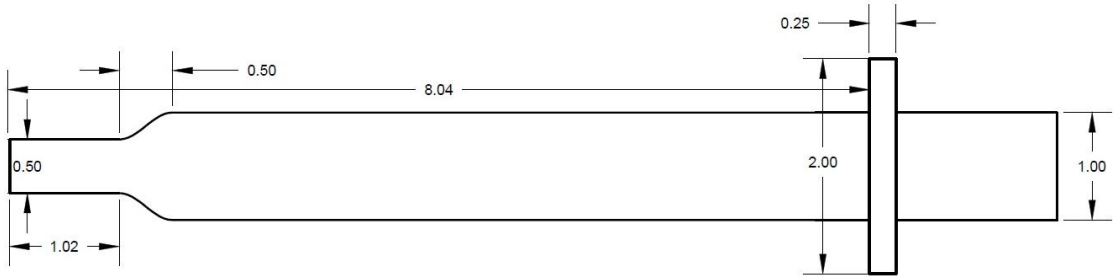

Figure 27 Schematic of quartz torch used for disinfection experiments. *(All dimensions are in inches.)*

3.5. Experimental Procedure

The plasma gas effluents flow downstream through the quartz torch and are bubbled through water contaminated by *Bacillus globigii* spores for a period of 30 minutes. In

order to maintain homogeneity of the solution, beaker was placed on a magnetic stirrer and the solution was stirred during the entire course of the experiment.

While the plasma system was in operation, an optical emission spectrometer (OES, from Ocean Optics, model number: HR4000CG-UV-NIR) was connected to the plasma system using an optical cable to observe the electromagnetic radiation generated by the plasma. The spectra are beneficial in observing the EM radiation generated and determining the effect on *B. globigii* spores. A residual gas analyzer (RGA, from Stanford Research Systems, model number: RGA – 300) was used to analyze the plasma effluent gases.

Every 10 minutes, 10 mL solution was drawn from the beaker using pipette and transferred into a sterile vial. A small volume of the collected sample was analyzed using inductively coupled plasma – optical emission spectroscopy (ICP-OES, from PerkinElmer Optima, model number: 2100 DV).

3.6. Quantitatively estimating extent of water disinfection

After the experiment, the collected samples were serially diluted in sterile vials. Each vial was vigorously stirred using a vortex mixer before spreading 0.1 mL of solution from it. The solution was spread uniformly on Trypticase Soy Agar (TSA) plates. The plates were then covered and flipped to avoid loss of water; they were then incubated at 37°C for a period of 24 hours.

Spread plating and counting was done based on the procedure described in section 9215B.[57] Post incubation, the number of colonies on each plate were counted. Based on the average number of colonies for each dilution, an estimate of the average number of spores remaining in the beaker after 10, 20 and 30 minutes of treatment was made. Following example illustrates the procedure for counting the number of colonies in the beaker at any given point of time.

Assuming:

Concentration of spores in beaker after treating for 20 minutes = x cfu/mL

10 mL sample was drawn from the beaker and serially diluted. The diluted samples were spread on TSA plate. After 24 hours incubation at 37 °C, following results were observed:

Sample 1: Undiluted sample results in 400 colonies

Sample 2: 10^{-2} dilution results in 76 colonies

Sample 3: 10^{-4} dilution results in 2 colonies

Sample 4: 10^{-6} dilution results in 0 colonies

As per the Standard Methods – 9215 Heterotrophic Plate Count, [57] the number of spores is estimated by considering the number of colonies as 76. So the number of spores in the beaker = (No. of colonies) / (dilution ratio)^2 = 76/(10^{-2})^2 = 7.6 X 10^5 cfu/mL.

4. Results and Discussions

Figure 28 shows TSA plates covered with colonies of *Bacillus globigii*.

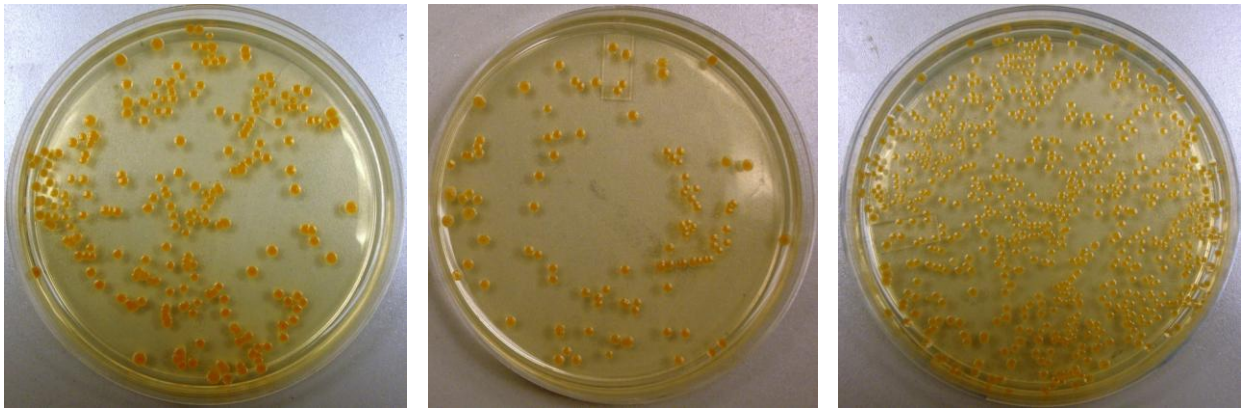

(a) (b) (c)

Figure 28 Colonies of Bacillus globigii spores on TSA plates after 24 hours of incubation at 37°C. (a, b) Plates with colonies between 30 – 300, (c) Plate with colonies greater than 300.

Figure 29 graphically represent the ratio of viable spores to original number of spores in water treated with plasma effluents from He-H_2 and He plasma at different generator power levels. The flow rate of gas was kept constant at 3000 sccm. A flow rate of 3000 sccm was optimum to ensure that the plasma sustained itself for all the gases without getting extinguished midway through the experiment. If the flow rate was increased beyond 3000 sccm, water from the beaker started spattering around the setup.

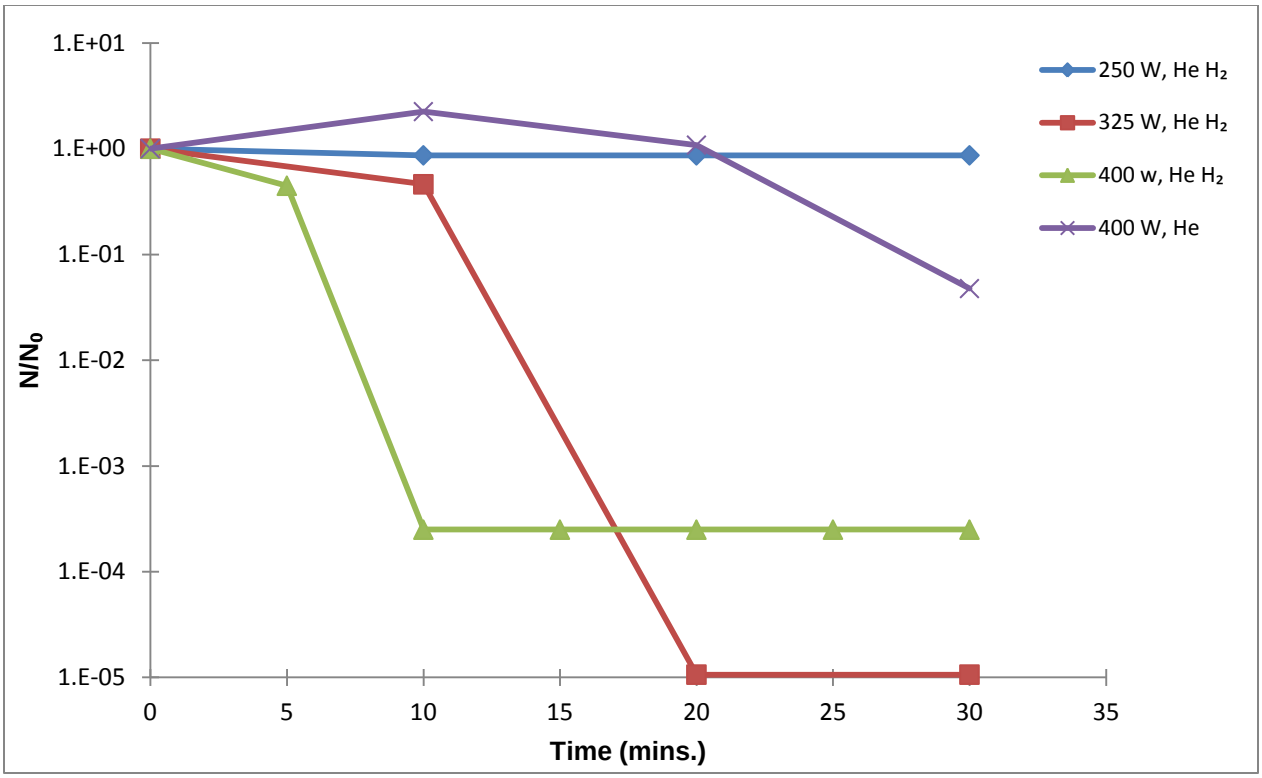

Figure 29 Disinfection results of water sample contaminated by *B. globigii* treated with plasma effluents. Flow rate of He-H_2 and He was kept constant at 3000 sccm and the plasma system was operated at varying power levels.

Helium being a noble gas has very high ionization energy. Therefore, it is unlikely that helium plasma generates significant amount of reactive species[54] that contribute towards eradication of *Bacillus* spores.

On the other hand, when 1% H_2 was added to He and the generator power is set to 325 – 400 W, disinfection is significant with 30 minutes of plasma application.

In order to understand the cause of disinfection, optical emission spectra of the EM radiation of He and He-H_2 as the plasma was obtained. Figure 30 shows an overlap of the spectra generated by the two plasmas. The plasma generated by He-H_2 gas mixture produces very strong UV radiation in the range of 200-300 nm.

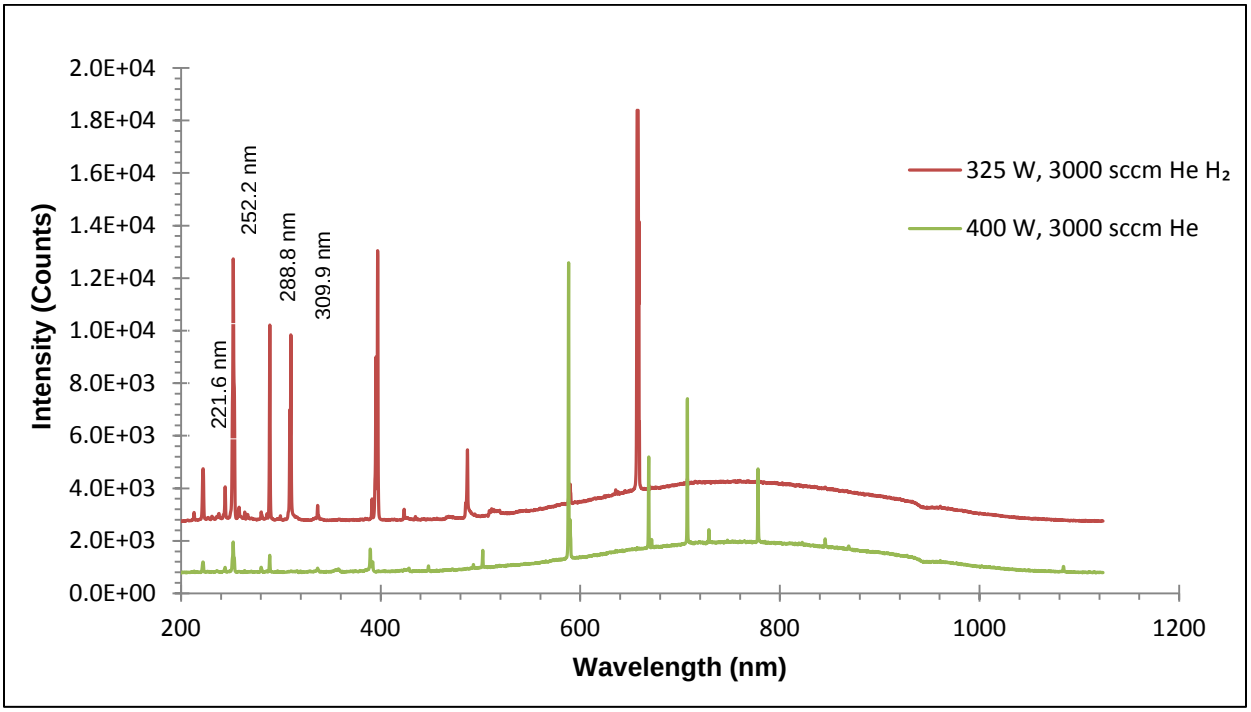

Figure 30 OES spectra of plasma generated by He-H_2 and He gases. The operating parameters of the plasma system are mentioned in the legend.

Based on the literature survey, it is evident that UV radiation and resulting OH radicals are responsible for eradication of *B. globigii* spores. UV radiation breaks down the chemical bonds in the spores resulting in formation of volatile compounds like CO and CH_x, which kills the bacteria. Alternatively, UV can also damage the DNA helices of the spore beyond repair, thus leading to its death.[51, 58]

The cell membrane of the bacteria consists of a lipid bilayer with embedded protein molecules. The lipid membranes, which are essentially made up of fatty acids, control the transport of ions and polar compounds into and from the cells. The OH radicals generated by the plasma react with the lipid bilayer membrane of the B. globigii bacteria, thus damaging the unsaturated fatty acids and oxidizing the embedded protein.[59] As a result, nucleic acids, lipids, proteins and sugars in bacteria are converted to carbonyl compounds and cause deamidation, racemization, and isomerization of protein residues,[48] resulting in protein degradation and cell inactivation.

Disinfection of *B. globigii* spores using oxygen as the plasma gas was successful. Figure 31 graphically compares the efficiency of plasma effluents from O_2 and N_2 plasma (at different generator power levels) in disinfecting water contaminated by *B.globigii* spores. The flow rate of gas was kept constant at 3000 sccm.

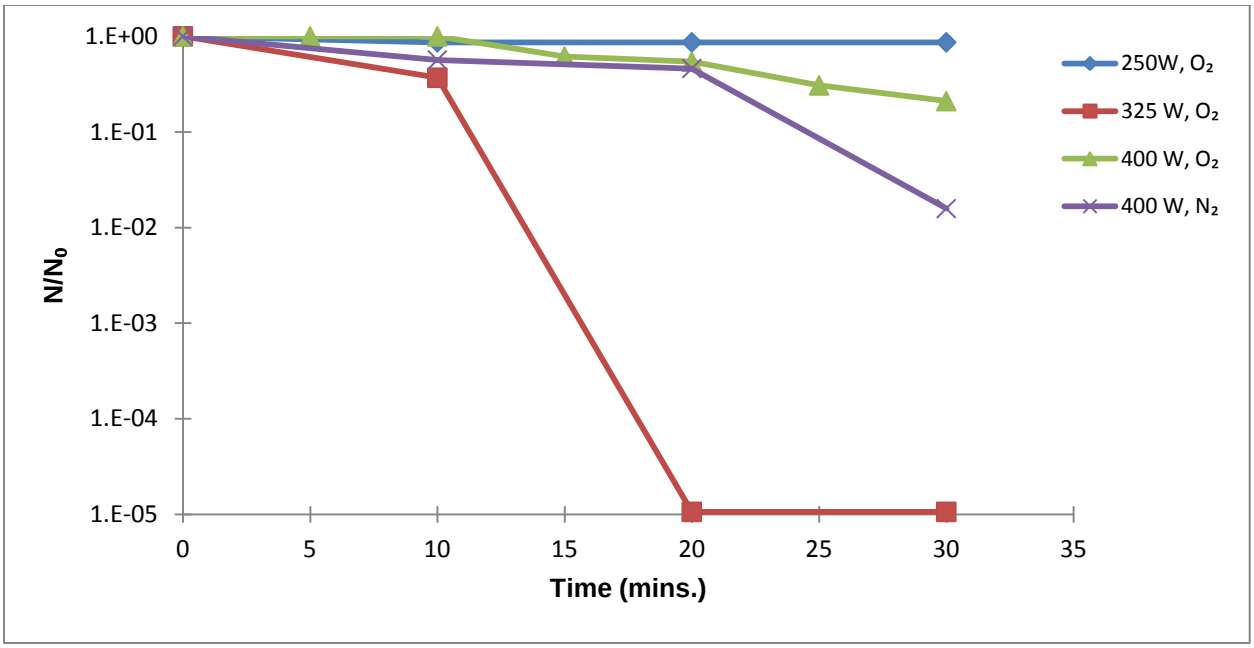

Figure 31 Disinfection results of water sample contaminated by *B. globigii* treated with plasma effluents. Flow rate of O_2 and N_2 was kept constant at 3000 sccm and the plasma system was operated at varying power levels.

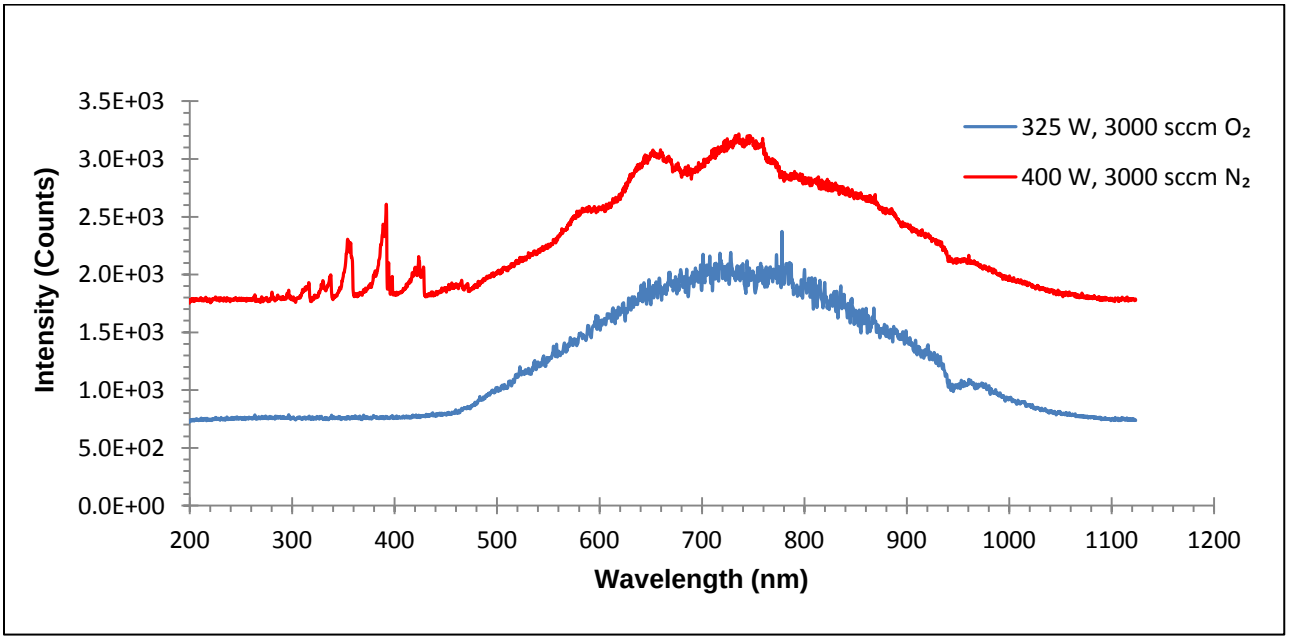

Figure 32 OES spectra of plasma generated by O_2 and N_2 gases. The operating parameters of the plasma system are mentioned in the legend.

Based on the above results, it is evident that *B. globigii* spores are eradicated when the plasma system is operated at 325 W and 400 W and 3000 sccm of oxygen flow rate.

Plasma systems that use oxygen as the plasma gas produce reactive oxygen species (ROS) such as O radicals, singlet molecular oxygen (a $^1\Delta_g$), ozone (O_3) and superoxide (O_2^-) and hydroxyl radicals (OH).[9, 48, 53]

Moreau *et al* suggest that oxygen radicals gets chemisorbed on the surface of the bacteria and they react with the cell membrane to form CO_2.[51] As a result, the oxygen radicals oxidize the membrane, thus leading to cell death. Another possible mechanism of bacterial death could be due to ozone. Thus, one or more of the above mentioned reactions can explain death of *B. globigii* spores.

In order understand the effect of pH on disinfection of spores, disinfection experiments were carried out with nitrogen as the plasma gas. After 30 minutes of treatment, the pH of the water solution decreased from 6.5 to 3.5 due to dissolution of NO and NO_x species. However no significant disinfection was observed, contrary to the work of Laroussi *et al.*[8]

RGA was used to analyze the composition of the plasma effluent gases.

Figure **33** shows various peaks observed from the scan and probable fragments that may result into these peaks.

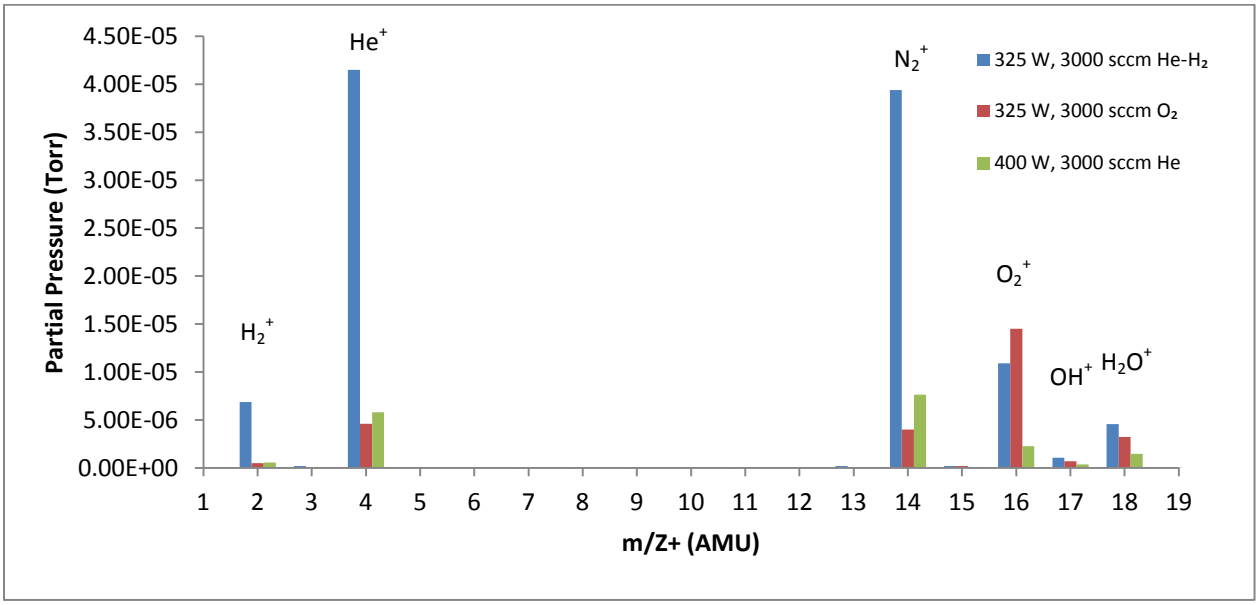
4.50E-05
4.00E-05
3.50E-05
3.00E-05
2.50E-05
2.00E-05
1.50E-05
1.00E-05
5.00E-06
0.00E+00
Partial Pressure (Torr)
1 2 3 4 5 6 7 8 9 10 11 12 13 14 15 16 17 18 19
m/Z+ (AMU)
He+
N2+
O2+
H2+
OH+
H2O+
325 W, 3000 sccm He-H2
325 W, 3000 sccm O2
400 W, 3000 sccm He

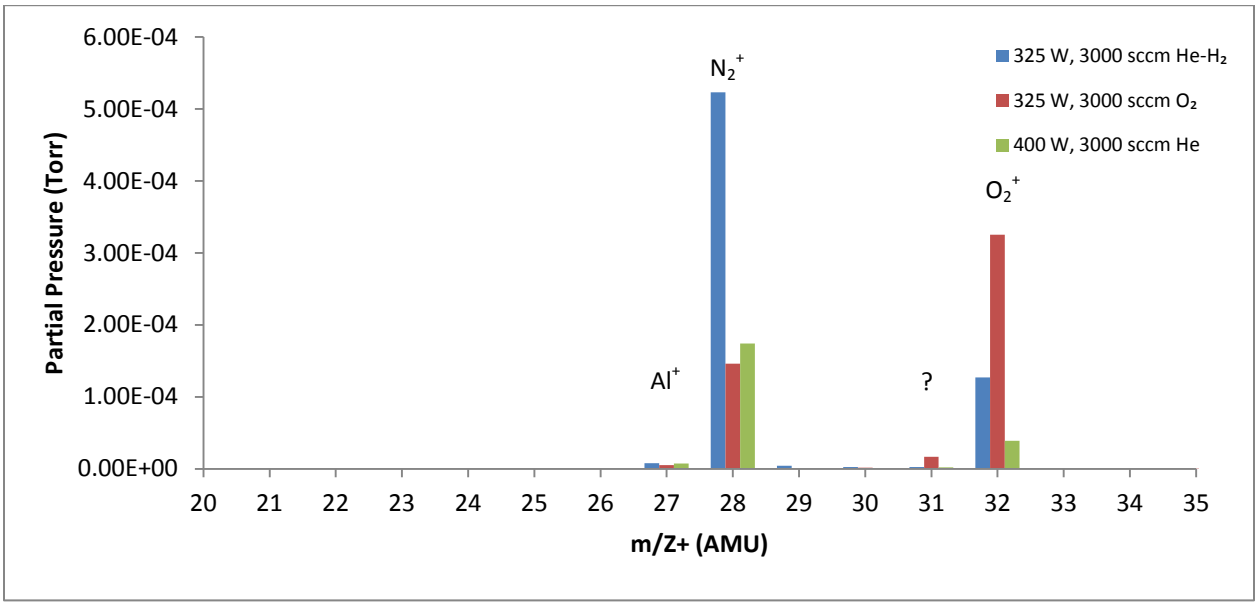
6.00E-04
5.00E-04
4.00E-04
3.00E-04
2.00E-04
1.00E-04
0.00E+00
Partial Pressure (Torr)
20 21 22 23 24 25 26 27 28 29 30 31 32 33 34 35
m/Z+ (AMU)
N2+
O2+
Al+
?
325 W, 3000 sccm He-H2
325 W, 3000 sccm O2
400 W, 3000 sccm He

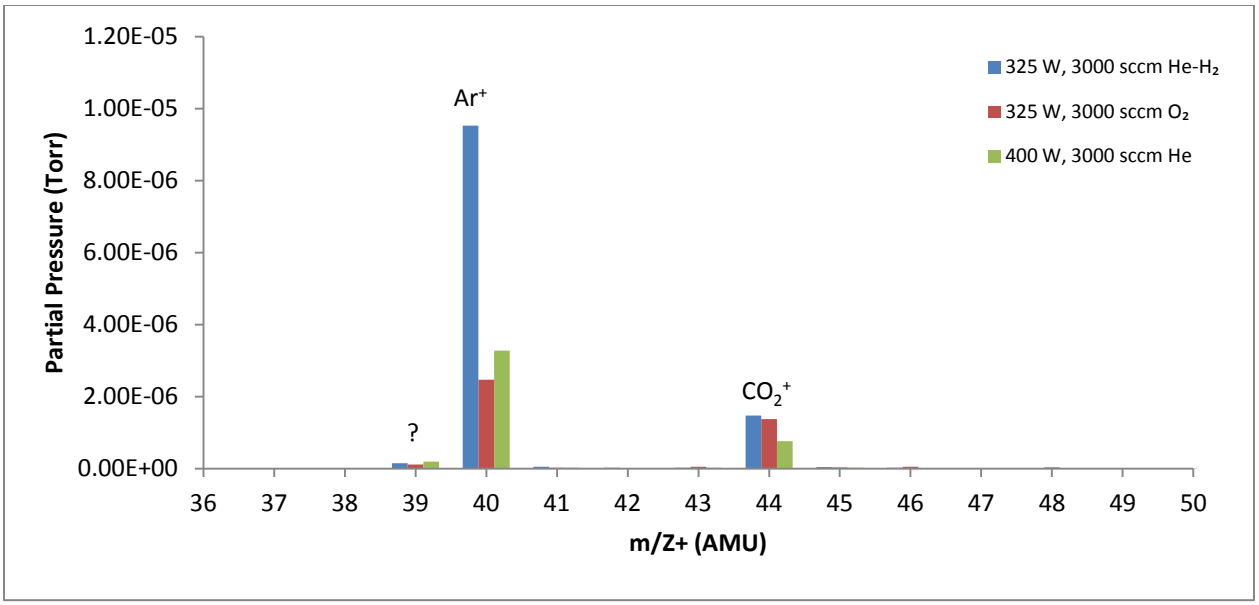

Figure 33 RGA data of plasma effluents produced from different plasma gases.

Peaks may arise due to decomposition of alumina rod, which is present at the center of microwave plasma cavity. High temperature at the core of plasma causes the alumina to decompose and dissolve in water during the course of the experiment. Since the rod is responsible for generating plasma, it cannot be eliminated from the system.

Literature review of mass spectra [60] along with ICP-OES of water samples confirms that the alumina from the rod is decomposed and gets carried with the plasma effluents. The change in concentration of aluminum dissolved in water with time has been graphically represented in

Figure **34**.

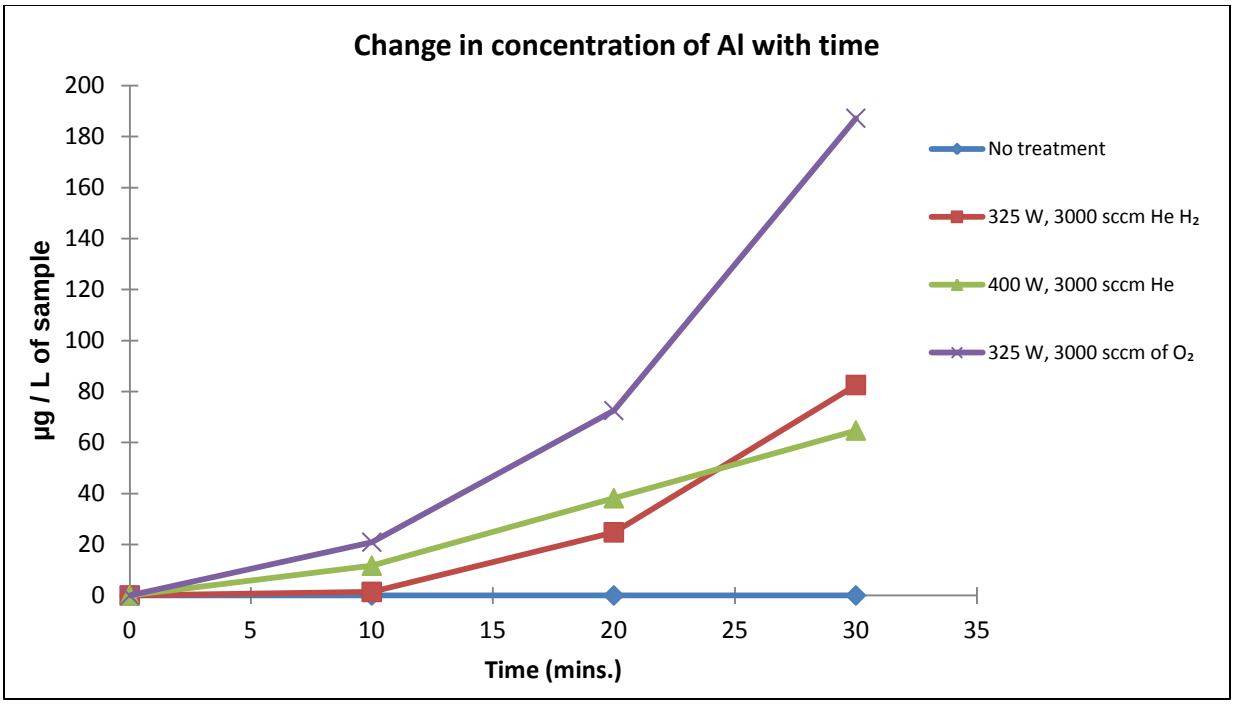

Figure 34 Change in concentration of Aluminum dissolved in water with time.

Literature survey suggests that presence of alumina micro and/or nano particles in water can also partly contribute to disinfection of water.[61, 62] However, the contribution of alumina micro and/or nano particles towards disinfections remains inconclusive.

5. Conclusions

A. Atmospheric pressure microwave plasma system can be successfully used to treat water contaminated by B*acillus globigii* spores.

B. Among the four gases (He + 1% H_2, He, O_2, N_2), best disinfection was obtained with O_2 and He + 1% H_2.

C. Complete disinfection of water was observed when the power level of magnetron was set to 325W and 400 W.

D. Plasma generated with He-H_2 as plasma gas is a rich source of H radicals and UV radiation. These factors cause disinfection of Bacillus globigii species in water. On the other hand, O_3, ROS and OH radicals can be considered as the main disinfecting agents for oxygen plasma.

E. Thus, a combination of UV and ROS is a credible method to decontaminate water contaminated by bacteria.

References

1. A. Grill, *Cold Plasma Materials Fabrication: From Fundamentals to Applications*. (John Wiley & Sons, 1994).
2. Y. Hayashi, T. Fukumura, K. Odani, T. Matsuba and R. Utsunomiya, Thin Solid Films **518** (13), 3506-3508 (2010).
3. H. Griffiths, C. Xu, T. Barrass, M. Cooke, F. Iacopi, P. Vereecken and S. Esconjauregui, Surface and Coatings Technology **201** (22–23), 9215-9220 (2007).
4. C. Bower, W. Zhu, S. Jin and O. Zhou, Applied Physics Letters **77** (6), 830-832 (2000).
5. Z. F. Ren, Z. P. Huang, J. W. Xu, J. H. Wang, P. Bush, M. P. Siegal and P. N. Provencio, Science **282** (5391), 1105-1107 (1998).
6. P. W. May, Philosophical Transactions of the Royal Society of London. Series A: Mathematical, Physical and Engineering Sciences **358** (1766), 473-495 (2000).
7. D. Pappas, Journal of Vacuum Science & Technology A: Vacuum, Surfaces, and Films **29** (2), 020801-020817 (2011).
8. M. Laroussi, Ieee Transactions on Plasma Science **30** (4), 1409-1415 (2002).
9. H. W. Herrmann, I. Henins, J. Park and G. S. Selwyn, Physics of Plasmas **6** (5), 2284-2289 (1999).
10. C. Sarra-Bournet, S. Turgeon, D. Mantovani and G. Laroche, Plasma Processes and Polymers **3** (6-7), 506-515 (2006).
11. V. Andreas, O. Andreas, F. Rüdiger, S. Karsten and W. Klaus-Dieter, Journal of Physics D: Applied Physics **43** (48), 485201 (2010).

12. E. Abadjieva, A. E. D. M. van der Heijden, Y. L. M. Creyghton and J. R. van Ommen, Plasma Processes and Polymers **9** (2), 217-224 (2012).
13. V. Shanov, S. Datta, F. Miralai and J. McDaniel, United States, Patent No. 6841201 (2005).
14. ASTEX, SmartMatch^{TM} manual, 1997 Revision D.
15. T. W. Ebbesen, Physics Today **49** (6), 26-32 (1996).
16. M. Mao and A. Bogaerts, Journal of Physics D: Applied Physics **43** (31), 315203 (2010).
17. K. Donaldson, R. Aitken, L. Tran, V. Stone, R. Duffin, G. Forrest and A. Alexander, Toxicological Sciences **92** (1), 5-22 (2006).
18. R. Pfeiffer, T. Pichler, Y. Kim and H. Kuzmany, (Springer Berlin / Heidelberg, 2008), Vol. 111, pp. 495-530.
19. M. M. J. Treacy, T. W. Ebbesen and J. M. Gibson, Nature **381** (6584), 678-680 (1996).
20. C. Jayasinghe, W. F. Li, Y. Song, J. L. Abot, V. N. Shanov, S. Fialkova, S. Yarmolenko, S. Sundaramurthy, Y. Chen, W. D. Cho, S. Chakrabarti, G. Li, Y. Yun and M. J. Schulz, MRS Bull. **35** (9), 682-692 (2010).
21. S. R. Bakshi, D. Lahiri and A. Agarwal, International Materials Reviews **55** (1), 41-64 (2010).
22. A. Gohier, T. M. Minea, S. Point, J. Y. Mevellec, J. Jimenez, M. A. Djouadi and A. Granier, Diamond and Related Materials **18** (1), 61-65 (2009).
23. N. Li, Y. Huang, F. Du, X. He, X. Lin, H. Gao, Y. Ma, F. Li, Y. Chen and P. C. Eklund, Nano Letters **6** (6), 1141-1145 (2006).

24. F. Ko, Y. Gogotsi, A. Ali, N. Naguib, H. Ye, G. L. Yang, C. Li and P. Willis, Advanced Materials **15** (14), 1161-1165 (2003).
25. M. Zhang, K. R. Atkinson and R. H. Baughman, Science **306** (5700), 1358-1361 (2004).
26. D. Shi, J. Lian, P. He, L. M. Wang, F. Xiao, L. Yang, M. J. Schulz and D. B. Mast, Applied Physics Letters **83** (25), 5301-5303 (2003).
27. L. Li, N. Bowler, S. H. Yoon and M. R. Kessler, *Dielectric Properties of PTFE Wiring Insulation as a Function of Thermal Exposure*, presented at the Electrical Insulation and Dielectric Phenomena, 2008. CEIDP 2008. Annual Report Conference on, 2008.
28. G. H. Yang, S. W. Oh, E. T. Kang and K. G. Neoh, Journal of Vacuum Science & Technology A: Vacuum, Surfaces, and Films **20** (6), 1955-1963 (2002).
29. V. Kumar, J. Pulpytel and F. Arefi-Khonsari, Plasma Processes and Polymers **7** (11), 939-950 (2010).
30. A. Hirsch and O. Vostrowsky, edited by A. D. Schlüter (Springer Berlin / Heidelberg, 2005), Vol. 245, pp. 193-237.
31. Q. Chen, L. Dai, M. Gao, S. Huang and A. Mau, The Journal of Physical Chemistry B **105** (3), 618-622 (2000).
32. N. O. V. Plank, L. Jiang and R. Cheung, Applied Physics Letters **83** (12), 2426-2428 (2003).
33. Z. N. Utegulov, D. B. Mast, P. He, D. Shi and R. F. Gilland, J. Appl. Phys. **97** (10), 104324-104324 (2005).
34. H. Yasuda, *Plasma polymerization*. (Academic Press, Inc., 1985).
35. K. Young Jo, M. Hongbin and Y. Qingsong, Nanotechnology **21** (29), 295703 (2010).

36. S. Eofinger, W. J. van Ooij and T. H. Ridgway, Journal of Applied Polymer Science **61** (9), 1503-1514 (1996).
37. S. Gaur and G. Vergason, *Plasma Polymerization:Theory and Practice*, presented at the 43rd Annual Technical Conference Proceedings, Denver, 2000.
38. M. J. Schulz, V. N. Shanov and Y. Yun, *Nanomedicine Design of Particles, Sensors, Motors, Implants, Robots, and Devices*. (Artech House, 2009).
39. C. Jayasinghe, S. Chakrabarti, M. J. Schulz and V. Shanov, Journal of Materials Research **26** (05), 645-651 (2011).
40. E. J. Kinmond, S. R. Coulson, J. P. S. Badyal, S. A. Brewer and C. Willis, Polymer **46** (18), 6829-6835 (2005).
41. S. J. Lue, S.-Y. Hsiaw and T.-C. Wei, Journal of Membrane Science **305** (1–2), 226-237 (2007).
42. F. F. Shi, Surface and Coatings Technology **82** (1–2), 1-15 (1996).
43. D. Briggs, A. Brown and J. C. Vickerman, *Handbook of Static Secondary Ion Mass Spectrometry*. (J. Wiley, 1989).
44. J. H. Kwon, S. W. Youn and Y.-C. Kang, Bulletin of the Korean Chemical Society **27** (11), 1851-1853 (2006).
45. J. Riddle, *SEMASPEC Test Method for XPS Analysis of Surface Composition and Chemistry of Electropolished Stainless Steel Tubing for Gas Distribution System Components*, 1993.
46. A. A. Hosni, J. G. Szabo and P. L. Bishop, J. Environ. Eng.-ASCE **137** (7), 569-574 (2011).

47. C. Solazzo, D. Erhardt, F. Marte, D. von Endt and C. Tumosa, Applied Physics A: Materials Science & Processing **79** (2), 247-252 (2004).
48. W. S. Lai, H. R. Lai, S. P. Kuo, O. Tarasenko and K. Levon, Physics of Plasmas **12** (2) (2005).
49. W. D. Burrows and S. E. Renner, Environ. Health Perspect. **107** (12), 975-984 (1999).
50. G. Irving, T. McMurray and J. Herbold, *Non-medical dispersed biological weapons countermeasures*, 1997.
51. S. Moreau, M. Moisan, M. Tabrizian, J. Barbeau, J. Pelletier, A. Ricard and L. Yahia, J. Appl. Phys. **88** (2), 1166-1174 (2000).
52. *Ultraviolet Disinfection Guidance Manual For the Final Long Term 2 Enhanced Surface Water Treatment Rule*, November 2006.
53. S. Williams, S. Popovic and M. Gupta, Plasma Sources Sci. Technol. **18** (3) (2009).
54. H. Shintani, A. Sakudo, P. Burke and G. McDonnell, Experimental and Therapeutic Medicine **1** (5), 731-738 (2010).
55. J. G. Szabo, E. W. Rice and P. L. Bishop, Applied and Environmental Microbiology **73** (8), 2451-2457 (2007).
56. C. R. Harwood and S. M. Cutting, (Wiley, 1990), pp. 391–429.
57. A. D. Eaton, L. S. Clesceri and A. E. Greenberg, (American Public Health Association, American Water Works Association, Water Environment Federation, 1995).
58. N. Philip, B. Saoudi, M. C. Crevier, M. Moisan, J. Barbeau and J. Pelletier, Ieee Transactions on Plasma Science **30** (4), 1429-1436 (2002).

59. M. Laroussi and F. Leipold, International Journal of Mass Spectrometry **233** (1-3), 81-86 (2004).
60. M. Novotny, J. Bulir, J. Lancok, P. Pokorny and M. Bodnar, J. Nanophotonics **5** (2011).
61. S. Pakrashi, S. Dalai, D. Sabat, S. Singh, N. Chandrasekaran and A. Mukherjee, Chem. Res. Toxicol. **24** (11), 1899-1904 (2011).
62. W. Jiang, H. Mashayekhi and B. S. Xing, Environ. Pollut. **157** (5), 1619-1625 (2009).

Future Work

A. Materials processing:

a. Functionalized CNT ribbons will be incorporated as reinforcement in light weight polymer composites. The mechanical characterization of these samples will be carried out to study the change in mechanical properties of the composites.

b. Since the effluent gas temperature of RF plasma system is observed to be lower than that of microwave plasma system, RF plasma system (shown in Figure 35) will be used for functionalization of ribbons before incorporating them into composites. Based on mechanical characterization of these samples, conclusion would be drawn about the effectiveness of the two plasma systems in functionalization of CNT ribbons.

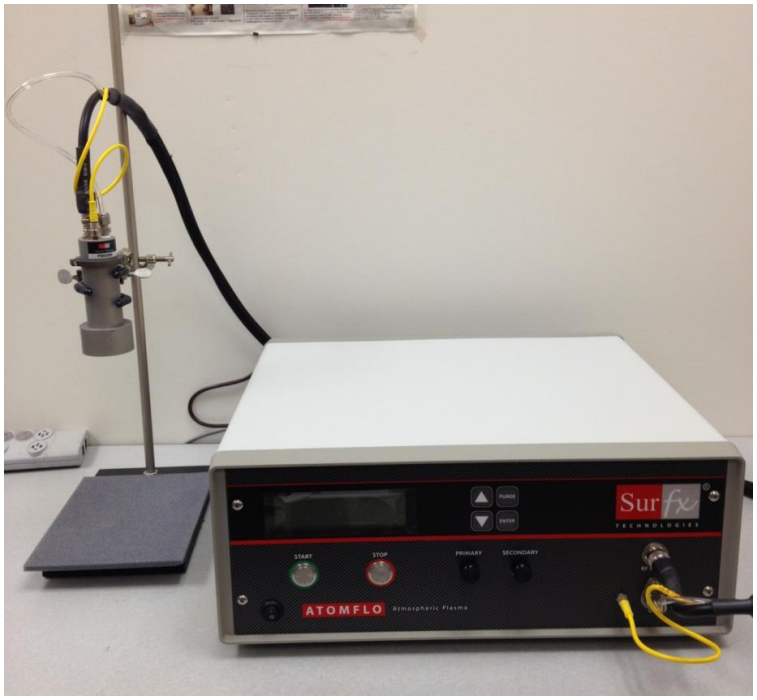

Figure 35 Atmospheric pressure RF plasma system from Atomflow 400D from Surfx Technologies.

c. In order to form an insulating coating over CNT ribbons, they will be first functionalized by plasma. This may improve the adhesion of consecutive layers of polymers with the surface of CNT ribbons.

B. Environmental Applications

a. Disinfection of water contaminated with *B. globigii* spores will be carried out using the Surfx plasma system (Figure 35). Based on the results obtained, the effectiveness of the two plasma system can be established.

b. Solid surfaces contaminated by *B. globigii* spores can be treated by the Surfx plasma system for duration of 30 minutes. Based on the number of viable spores after the treatment, conclusions can be drawn about the effectiveness of Surfx plasma system for decontaminating solid surfaces.